TRANSITION IN THE WAKE OF A SMALL CIRCULAR CYLINDER ATTACHED TO A FLAT PLATE

A.K. GUPTA

DEPARTMENT OF AEROSPACE ENGINEERING
INDIAN INSTITUTE OF TECHNOLOGY KANPUR

JULY 1991

DEPARTMENT OF AEROSPACE ENGINEERING
INDIAN INSTITUTE OF TECHNOLOGY KANPUR

TRANSITION IN THE WAKE OF A SMALL CIRCULAR CYLINDER ATTACHED TO A FLAT PLATE

A.K. GUPTA

Department of Aerospace Engineering
Indian Institute of Technology Kanpur

STRACT

An experimental investigation was conducted at a wind speed 4.1 m/sec to study the details of transition in the wake of cular cylinder of diameter 3.1 mm and of the same height tically attached to a flat plate at a distance of 30 cm from leading edge, and immersed in the laminar boundary layer of ckness 4.2 mm. Reynolds number based on cylinder height and placement thickness were 827 and 384, respectively. Extensive a using a single hot wire probe were collected up to a distance 80 diameters downstream of the cylinder. Detail results wed that the onset of turbulence in the cylinder wake was ceded by strong vortex ring shedding like flow structure. near wake appeared to possess a two layer vertical structure; er wake region where the disturbances decayed downstream, and inner wall layer where the disturbances were growing in the -lobe regions.

Introduction

Fluid flows undergo transition from laminar to turbulent state as the Reynolds number is increased. In addition to Reynolds number, transition depends also on free stream turbulence level, body forces, pressure gradient in the flow direction, and the conditions at the boundary like the roughness, temperature and velocity. Because of the simplicity and fundamental nature, transition of the laminar boundary layer on a flat plate has been investigated quite extensively by Schlichting (1960), Schubauer and Skramstad (1947), Klebanoff, Tidstrom and Sargent (1962), Benney ad Lin (1960), Emmons (1951). As a result, the physical mechanism of boundary layer natural transition are well understood and established.

On the other hand, quite often wind tunnel engineers mount roughness elements near the leading edge or nose of the wind tunnel models as artificial tripping devices to promote earlier onset or to fix transition and thereby have turbulent flow over most of the wetted surface of the model. Basically there are three types of artificial tripping devices or roughness elements like a thin wire or ring used by Prandtl in his classical experiment on sphere drag, three dimensional roughness elements like a row of spheres, or cones, or circular cylinders, and grit type roughness elements like sand paper or emery paper. Empirical correlations for low speeds between the height of the roughness element, its location and transition Reynolds number have been obtained Klebanoff, Schubauer & Tidstrom (1955), Potter (1957), Dryden (1959), Smith & Clutter (1959), and Tani (1969).

These provide necessary information to select suitable sizes of roughness elements for fixing the transition location. However, the physical mechanism by which an artificial tripping device brings an earlier onset of transition has been studied for the case of the two dimensional roughness element only recently. The experimental investigation of Klebanoff and Tidstrom (1972) has shown that the earlier transition due to a two dimensional roughness element is stability governed phenomenon. While the disturbances introduced by the two dimensional tripping device decay as they travel downstream, the mean flow field in the near wake of the two dimensional roughness element features inflexional type mean velocity profiles which are much more destabilising than the Blasius type velocity profile. As a result Tollmien-Schlichting type disturbances amplify at a much faster rate culminating in an earlier onset of transition.

The mechanism of transition due to three dimensional roughness elements is believed to be more critical in nature than that of a two dimensional roughness element. Until a critical velocity or a critical roughness element Reynolds number is attained the presence of a row of circular cylinders or spheres does not affect the transition. Further slightest increases in the free stream velocity or roughness element height attaches the transition to the tripping device location, and turbulence wedges appear some distance downstream of the roughness elements. This critical roughness element Reynolds number lies in a narrow range of 600-1000, as observed by Klebanoff, Schubauer and Tidstrom (1955), and Tani, Komoda, Komatsu and Iuchi (1962).

Since the transition in the wake of a sphere placed in a uniform flow appears in about the same Reynolds number range, it is believed that the transition becomes attached as soon as the wake of the three dimensional roughness element has become turbulent. Mochizuki (1961) has carried out an experimental investigation of smoke flow visualization in the wake of a sphere attached to a flat plate. These show an interesting range of phenomena including the appearance of turbulence wedge preceded by vortex ring shedding like periodic flow structure. Hall (1967) has studied the interaction of the wake from a truncated small circular cylinder as it is mounted at different vertical locations inside a laminar boundary layer, while Sedney (1973) has written a survey of the effect of small protuberances on boundary layer flows. Transition in the sphere wake for Reynolds number less than 1000 has been investigated by means of flow visualisation techniques by Taneda (1956), Magarvey and Bishop (1961), Magarvey and MacLatchy (1965), and Achenbach (1974).

The present experimental investigation was undertaken with the objective of studying the wake of an isolated three dimensional roughness element like a vertical small circular cylinder attached to a flat plate and immersed in the laminar boundary layer with a view to clarify further the physical mechanism of laminar boundary layer transition due to three dimensional roughness element. The set up and test conditions were similar to those of Mochizuki (1961) except for two major differences. These were: a circular cylinder and hot wire technique in the present investigation in contrast to a sphere and

smoke flow visualisation technique in Mochizuki's investigation. In the present investigation, detail flow surveys up to 80 diameters were made in the wake of the circular cylinder roughness element with a single hot wire. Preliminary results of this investigation have been reported earlier and detail results which form the present paper were presented in ICTAM-80 by Gupta (80).

2. Experimental Set-up and Procedure

2.1 Low Turbulence Wind Tunnel

The experiments were carried out in an open circuit suction type low speed low turbulence wind tunnel with a contraction ratio of 16 and a test section size of 0.6m x 0.6m x 3.1 m. The turbulence level as measured with a single wire probe was about 0.2% at a nominal wind speed of 4 m/sec. The tunnel was fitted with a DC motor-propeller fan combination . The RPM of the propeller fan shaft was monitored on a tachogenerator driven voltmeter during all tests.

The test section had plexiglass side walls and a wooden top wall with a cut out of 20 cm width and 80 cm length to enable the probe to traverse the plate surface in all the three directions. Appropriate size wooden plugs were made to cover the slot everywhere except the region of probe location. Two aluminium railings were fitted on the roof of the test section parallel to the flat plate length on which three translational degrees of freedom traversing mechanism was mounted. The maximum distances which could be traversed in the stream wise, x,

rtical, y, and span wise, z directions were 45 cm, 15 cm and cm respectively. the distances in the x, y, and z directions re read on three mechanical digital counters which provided solutions of 0.125 mm, 0.05 mm, and 0.05 mm respectively.

2 Flat Plate and the Circular Cylinder/3-D Tripping Device

An aluminium plate 1 cm thick x 60 cm wide x 2.4 m long was ounted horizontally in approximately the middle of the test ection height. The plate was machined on a horizontal planar and as hand lapped for a good surface finish. To increase the tiffness of the plate aluminium angle frames were attached to he bottom of the plate. To prevent leading edge separation, the eading edge was given an elliptical contour, a half wedge made f wood was attached to the bottom of the plate ahead of the luminum frame, and the plate was mounted 3 cm above the middle ine of the test section height. Plate leading edge details are hown in Fig. 1.

The smoke flow visualisation as well as hot wire signal races observed on the oscilloscope showed that the plate boundary ayer was laminar without traces of turbulent spots up to a listance of 1.5 m from the leading edge at a nominal wind speed f 4 m/sec. The circular cylinder of height and diameter qual to 3.1 mm was made out the head of a brass thin bolt ocated along the middle of the plate width at a distance of 30 m. downstream of the plate leading edge. Details of he circular cylinder/tripping device and its mounting are hown in Fig. 1.

2.3. Hot Wire Probe and Anemometry Equipment

Miniature single hot wire probe was fabricated using jeweler's broaches of tip diameter 0.075 mm mounted with epoxy resin in a 3 mm diameter stem of the probe adjustable in a vertical tube of 1.25 cm diameter. The distance between the prong tips was about one third of a mm. Platinum core Wollaston type wire of 0.01 mm was soft soldered to the prong after etching. The ratios of the hot wire length to the wire diameter and to the circular cylinder diameter were 33 and 0.08, respectively.

A constant temperature hot wire anemometer DISA Model 55A01 was used extensively to measure stream wise velocity and disturbance intensities. The 'turbulent out' signal without filters was monitored continuously on a 545 B dual trace Tektronix oscilloscope. The spectra were measured on a General Radio wave analyzer Type 1900-A in the frequency range of 20 Hz - 20 KHz using the bandwidth ranges of 3 hz and 10Hz, ad were recorded on an X-Y recorder NE-2300. Electronic instruments were supplied with stabilized voltage to minimize disturbances from line frequency fluctuations.

2.4. Experimental Procedure and Data Analysis

Prior to data collection in the wake of the attached circular cylinder, the nature of the boundary layer on the clean plate was ascertained by making velocity measurements at discrete stream-wise and span-wise stations. After the check on two

dimensionality and the Blasius nature of velocity profile, the circular cylinder was mounted and detail surveys of mean streamwise velocity and disturbances intensities were made with the help of miniature hot wire probe. The streamwise stations downstream of the circular cylinder chosen for this purpose were $\hat{x}$ =1, 2, 3, 4, 6, 8, 12, 16, 24, 32, 48, 56, 64, 72 and 80, $\hat{x}$ is streamwise coordinate made nondimensional with the diameter of the circular cylinder and with its origin at the cylinder's vertical axis. At each streamwise station, the hot wire probe was traversed in the spanwise direction for different values of $\hat{y}$ in the range of 0 to 2, $\hat{y}$ is the vertical coordinate made nondimensional with the cylinder height and with its origin at the plate surface. Thus, there were typically about one hundred data points at each $\hat{x}$ station, the number of data points increasing at downstream x stations.

A simple procedure was adopted for calculation of mean streamwise velocity and disturbances intensities from the measured values of hot wire mean voltages E and rms voltage e' in volts. First, u'/U, the rms disturbance velocity normalised with local mean streamwise velocity was obtained using the following formula

$$\frac{u'}{U} = \frac{4\,E\,e'}{E^2 - E_o^2}$$

In this formula E_o is the hot wire voltage at zero wind speed which was recorded each time a wind tunnel run was made. E^2 was then corrected for drift in hot wire calibration by comparing E_o measured at the time of calibration. The corrected

E^2 provided $U^{1/2}$ from the calibration curve. Squaring of $U^{1/2}$ and normalising with U_∞, the free stream speed, resulted in U/U_∞, which upon multiplication with u'/U provided u'/U_∞.

3. Results and Discussion

For presenting the experimental results a rectilinear coordinate system x, y, z is defined with its origin at the base of the vertical cylinder axis; x coordinate downstream in the streamwise direction, y coordinate vertically up and z coordinate in the spanwise direction. The coordinates x, y z have been normalized with the height or diameter, 'd' of the cylinder, and are denoted by $\hat{x}$, $\hat{y}$, $\hat{z}$ respectively. Velocities, U and runs disturbance intensities, u', have been normalised with the free stream velocity U_∞.

The two dimensionality of the laminar boundary layer on the clean plate was checked by measuring U profiles at z = 0, ± 15 cm for two streamwise stations x = 0 and 60 cm. Fig. 2 shows the data plotted as y in mm vs U/U_∞. It is observed that the two-dimensionality is satisfactory at x = 0, and is tolerable at x = 60 cm. The boundary layer thickness has increased form about 4.2 mm at x = 0 to about 7.5 mm at x = 60 cm. The mean velocity data at the two 'x' stations corresponding to z = 0 are replotted in the Blasius coordinates as shown in Fig. 3. the data points corresponding to x = 0 fit the Blasius profile quite well, while those corresponding to x = 60 cm indicate slightly accelerating flow due to the boundary layer growth on the tunnel test section

walls. Figs. 2 and 3 together indicate that the laminar boundary layer over the clean plate at a free stream wind speed of 4.1 m/sec can be treated as reasonably good Blasius layer over the region of further experimentation.

For the purpose of reference the relevant flow parameters based on the air kinematic viscosity ν of 15.8 x 10-6 m^2/sec are reproduced in the following: Diameter d and height k each = 3.1 mm; streamwise distance of the circular cylinder from the leading edge x'_k = 30 cm; laminar boundary layer thickness δ = 4.2 mm at x'_k ; displacement thickness δ^* = 1.3 mm at x'_k; $\frac{k}{\delta}$ = 0.74; free stream wind speed U_∞ = 4.1 m/sec; streamwise velocity U_k = 0.92 U_∞ at x'_k and at vertical height k; Reynolds number $R_k = U_k\ k/\nu$ = 760; $R_d = U_\infty\ d/\nu$ = 827; $R_{\delta^*} = U_\infty\ \delta^*/\nu$ = 384; $R_{x'_k} = U_\infty\ x'_k/\nu$ = 7.95 x 10^4.

3.1 Nature of Disturbance on the Center Line; $\hat{z} = 0$; $\hat{y} = 1$

With the objective of determining qualitatively the manner of onset of transition, the hot wire probe was located on the center line of the wake of circular cylinder at $\hat{z} = 0$, $\hat{y} = 1$, and was traversed in the downstream direction so as to vary $\hat{x}$. The oscilloscope traces recorded at the sweep rate of 5 m sec/cm in the range of $1 \leq \hat{x} \leq 80$ are shown in Fig. 4.

It is observed that the hot wire signal does not indicate any disturbance for $\hat{x} \leq 2$. Then, at $\hat{x} = 3$ a weak sinusoidal wave form appears which is soon amplified to high levels for increasing $\hat{x}$. At $\hat{x} = 8$ the signal is spiky in nature with a

discrete disturbance frequency. the spikes are towards the low velocity side and appear to possess qualitative similarity with the spikes observed due to inflexional instability of hairpin eddies in flat plate boundary layer transition. For $\hat{x} > 8$ the spikes' intensity decreases while the wave form appears to change to incorporate the second harmonic within the predominant fundamental disturbances. For $\hat{x} > 56$ randomness typical of a turbulent signal appears to be creeping in, until at $\hat{x} = 80$ the presence of discrete disturbance can not be distinguished and the flow has become turbulent.

The frequency content of these hot wire signals shown in Fig. 4 was further probed with the help of a wave analyzer in the range of 20 Hz-1 KHz. Fig. 5 shows the typical spectra at about the same $\hat{x}$ locations as for the oscilloscope traces. Spectra corresponding to $\hat{x} = 1$ and 2 show no disturbance frequency content in agreement with the corresponding oscilloscope traces. A discrete frequency peak of about 220-240 Hz first appears at $\hat{x} = 3$ which increases in intensity at $\hat{x} = 4$ and 8. The smaller peak at a frequency of about 450-500 Hz which first appears at $\hat{x} = 4$ and persists for all subsequent values of $\hat{x}$ is more like the second harmonic of the disturbances. Very weak higher harmonics are also present in the spectra. At $\hat{x} = 56$, sub-harmonics of the fundamental and higher harmonics seem to appear while the spectrum corresponding to $\hat{x} = 64$ is acquiring the diffuse shape of the turbulent spectrum.

Some of these observations can be interpreted in the light of extensive smoke flow visualisation data obtained in the wake of a

spherical roughness element by Mochizuki (1961), and also reproduced by Sedney (1973). The strong discrete disturbances are quite likely to be the manifestation of periodic shedding of vortex rings. The values of Strouhal number for the vortex ring shedding turn out to be about 0.18 and 0.2 based on U_∞ and U_k, respectively. Achenbach (1974) has measured a Strouhal number of about 0.2 at Reynolds number of about 750 for a sphere placed in a uniform free stream water channel. Though it is not a two dimensional disturbance, one may calculate the quantity $2\pi f \delta^*/U_\infty$, which turns out to be about 0.54, a value well above the neutral stability boundary for Tollmien-Schlichting disturbances over a flat plate.

Results presented in Figs. 4 and 5 can be quantified by plotting u'/U_∞ vs $\hat{x}$. This plot is reproduced in Fig. 6 for easy reference from Gupta (1980). It is observed that u'/U_∞ increases first from $\hat{x} = 0$ to a peak value of about 10% near $\hat{x} = 8$ and then decreases to an almost constant value of 4% for $\hat{x} > 20$. The flow on the centerline of the wake at $\hat{y} \simeq 1$ appears to become turbulent for $\hat{x} \geq 64$. The data presented in Figs.4-6 were taken on different days, and in fact part of the data was collected by way of repetitive check after an interval of about a year. The details of transition were found to be quite sensitive to the wind tunnel fan RPM. A 5% alteration in fan RPM would result in a noticeable change of quantitative values of disturbance, its frequency and length of transition zone. However, the gross features of the transition phenomena remained the same reported in the foregoing.

3.2 Structure of Disturbances at $\hat{x} = 8.0$

The streamwise station $\hat{x} = 8.0$ is of interest because of the appearance of maximum rms intensity of the laminar disturbance in the vicinity as shown earlier. The distributions of U/U_∞ and u'/U_∞ vs $\hat{z}$ at different heights in the range of $1.8 \leq \hat{y} \leq 0.36$ are shown in Figs. 7 and 8. the salient aspect of the profiles in Fig. 7 is the high value of u'/U_∞ at $\hat{z} = 0$ in the range of $1.32 \leq \hat{y} \leq 0.84$, compared to relatively weak maxima of u'/U_∞ on either side of $\hat{z} = 0$ at $\hat{y} = 0.36$. Corresponding U/U_∞ profiles in Fig. 8 show velocity defect near $\hat{z} = 0$ whose magnitude decreases with increasing value of $\hat{y}$. Near the wall ($\hat{y} \cong 0.36$) the large undulations in U/U_∞ profiles are similar to those reported by Tani et al (1962) for the lower Reynolds number case, and are therefore due to a pair of longitudinal vortices attached to the plate.

Earlier experimental investigations of Mochizuki (1961), Tani et al (1962), Gregory & Walker (1956) and Sedney (1973) at lower Reynolds numbers have demonstrated a stationary state of laminar wake which consists of a pair of thin trailing longitudinal vortices in the outer wake region at $\hat{y} = 1.0$, and a pair of longitudinal vortices attached to the plate as part of the horse shoe vortex. The presence of horseshoe vortex has created a three dimensional mean flow in the form of a pair of longitudinal vortices in the laminar boundary layer. It may be recalled that measurements of Klebanoff et al (1962) have emphasised the appearance of three dimensional disturbances from initial two dimensional disturbances, which in turn cause the two dimensional mean flow to become three dimensional in the form of

longitudinal vortices. In the present case, three dimensionality of the mean flow is created locally by the circular cylinder wake and the horse shoe vortex before the appearance of noticeable laminar disturbances.

A set of typical hot wire traces recorded at the station $\hat{x}$ = 8 by traversing the hot wire probe in the vertical direction at $\hat{z}$ = 0 is shown in Fig. 9. There appears to be phase change in the disturbance across $\hat{y} \cong 1.16$, the disturbance magnitude decreases to a minimum value at about $\hat{y} = 0.4$. Similar hot wire traces recorded in the spanwise direction showed phase reversals on either side of $\hat{z} = 0$ at $\hat{y} = 1.0$, and spiky high magnitude traces spread over wider region of $\hat{z}$ at $\hat{y} = 0.2$. These features also indicate a vortex ring shedding like flow structure in the outer region near $\hat{y} = 1.0$, and another periodic flow structure in the inner wall region near $\hat{y} = 0.3$.

The mean velocity U/U_∞ and the disturbances rms intensity, u'/U_∞ profiles in the vertical direction for $\hat{x} = 8$ and two values of $\hat{z}$; $\hat{z}$ = 0 and 0.48 are shown in Fig. 10. At $\hat{z} = 0$, u'/U_∞ attains its peak value of about 14% at $\hat{y} = 1.2$. Furthermore, there is a likelihood of a second weaker maximum of u'/U_∞ appearing at $\hat{y} = 0.25$ as indicated by the hot wire traces in Fig. 9. u'/U_∞ profile corresponding to $\hat{z} = 0.48$ shows rms intensities to be less than 3% everywhere with the maximum appearing near $\hat{y}$ = 0.8. Corresponding U/U_∞ profiles show departures from Blasius profiles with velocity defect over most of the boundary layer height at $\hat{z} = 0$, and a smaller velocity excess at $\hat{z} = 0.48$.

3.3 Structure of Disturbances at $\hat{x} = 40$

Hot wire data at $\hat{x} = 40$ were obtained and plotted in the same manner as presented here for $\hat{x} = 8$. These have been reported earlier by Gupta (1980), Gupta and Singh (1979). The important results are the following:

The sharp peaks of u'/U_∞ at $\hat{z} = 0$ were not present at $\hat{x} = 40$. Instead, they were replaced by u'/U profiles with twin smaller peaks ($u'/U_\infty \cong 0.08$; $\hat{y} = 0.68$) at $\hat{z} = \pm 1.7$, with a valley ($u'/U_\infty \cong 0.05$; $\hat{y} \cong 0.68$) at $\hat{z} = 0$. Such u'/U_∞ profiles in the spanwise direction characterised by twin peaks symmetrically located off center of the wake, and a valley on the centerline of the wake, were present with varying degrees of magnitude at all vertical locations at $\hat{x} = 40$.

Hot wire traces at $\hat{x} = 40$ obtained by traversing the probe in the vertical direction $\hat{y}$, $\hat{z} = 0$, and in the spanwise direction $\hat{z}$ at $\hat{y} = 1.0$ showed persistence of laminar discrete frequency disturbance signal containing increased amount of higher harmonics with characteristic features like the phase reversal in the outer $\hat{y}$ and $\hat{z}$ regions similar to those shown here for $\hat{x} = 8$. Vertical profiles of u'/U_∞ were characterised by two maxima located as follows; $\hat{z} = 0$; $u'/U_\infty = 0.48$ at $\hat{y} = 1.2$ and $u'/U = 0.05$ at $\hat{y} = 0.3$; $\hat{z} = 1.44$; $u'/U_\infty = 0.06$ at $\hat{y} = 1.5$ and $u'/U_\infty = 0.09$ at $\hat{y} \simeq 0.7$. At $\hat{z} = -2.72$, u'/U was less than 0.02 at all $\hat{y}$.

These results indicate that the wake of a circular cylinder attached to the flat plate and immersed in the laminar boundary layer can be considered as made up of two layers in the $\hat{y}$

direction; an inner wall region bounded below by the plate having characteristics of wall shear flows, and an outer wake region near $\hat{y} = 1$, with characteristics similar to sphere wake. In the following, the data on the behaviour of disturbances in these two regions are presented for $1 \leq \hat{x} \leq 80$.

3.4 Growth of Disturbances in the Inner Region. $\hat{y} = 0.36$

The spanwise distributions of u'/U_∞ and U/U_∞ are shown in Figs.11 and 12, respectively.

Upto $\hat{x} = 2.0$, U/U_∞ profiles in Fig. 12 indicate the presence of cavity region where reverse flow occurs on the centerline as indicated by small hump at $\hat{x} = 1$. The velocity defect on the centerline is as high as $0.5\ U_\infty$. As shown in Fig. 11, u'/U_∞ disturbances have not appeared upto $\hat{x} = 2.0$, and these appear first at $\hat{x} = 3$ in a manner typical of disturbances intensity peaks in the two separated shear layers.

In the range of $3 \leq x \leq 80$ the following salient features of disturbances in the inner region are observed.

i) The maxima of disturbance rms intensities occur in the sidelobe regions at almost all $\hat{x}$ stations. Although, there are $\hat{x}$ stations in Fig. 11 like $\hat{x} = 16$, 32, 64 and 80 where comparable rms intensities occur at or near $\hat{z} = 0$ as well.

ii) The magnitudes of rms intensities in the side lobe region are increasing with distance downstream; from a value of $u'/U_\infty \cong 0.06$ occurring at $\hat{z} = \pm 0.3$, $\hat{x} = 4$ to $u'/U_\infty \cong 0.12$ occurring at $\hat{z} \pm 3$, $\hat{x} = 80$.

iii) The mean velocity profiles in Fig. 12 are characterised at each $\hat{x}$ station in the range $4 < \hat{x} < 32$ by symmetrically located twin velocity maxima near $\hat{z} = 0$ and twin velocity minima-further outwards from $\hat{z} = 0$. These profiles are characteristic of streamwise vortices.

iv) The velocity profiles corespoding to $\hat{x}$= 32, 40, and 48 in Fig. 12 indicate the appearance of additional streamwise vortices adjacent to the horseshoe streamwise vortices.

(v) For $\hat{x} = 64$ and 80 in Fig. 12, it appears that the appearance of turbulence is flattening the mean velocity spanwise profiles at these $\hat{x}$ stations.

3.5 Growth of Disturbances in the Outer Region: $\hat{y} = 1.0$

Figs. 13 and 14 show the u'/U_∞ and U/U_∞ vs $\hat{z}$ at different $\hat{x}$ stations in the outer wake region of the circular cylinder.

Again, the first sign of a weak disturbance ($u'/U_\infty < 0.02$) appears at $\hat{x} = 3$ as shown in Fig. 13. This disturbance grows very rapidly downstream to a value of $u'/U_\infty = 0.08$ within one diameter of the cylinder. This sharp single peak u'/U_∞ profiles

at $\hat{z} = 0$ decrease in magnitude for $\hat{x} > 8.0$. Compared to corresponding disturbance profiles in the inner region shown in Fig. 11, there is a basic difference in the character of two sets upto $\hat{x} < 16$; the outer region characterised by single high intensity peak at $\hat{z} = 0$ undergoing rapid change with $\hat{x}$, while the inner region characterised by twin peaks on either side of $\hat{z} = 0$ undergoing gradual increase in intensity. For stations $\hat{x} > 16$, u'/U_∞ profiles with two and three peaks appear with the sidelobe peaks generally not so intense as in the inner region.

The mean velocity profiles in Fig. 14 show in general the velocity defect near $\hat{z} = 0$. The undulations of mean velocity profiles in the outer region are not as pronounced as they have been observed in the inner region in Fig. 12. Comparing mean velocity profiles corresponding to $\hat{x} = 64$ and 80 (turbulent flow onset) in the inner (Fig. 12) and the outer (Fig. 14) region it is observed that in the outer region the man velocity near $\hat{z} = 0$ (turbulent flow) is less than the velocity at $\hat{z} > \pm 6$ (laminar flow), while in the inner region the reverse is the case. This fits very well with the existence of a turbulence wedge surrounded on either side by laminar boundary layer.

4. Summary and Conclusion

Based on the earlier experimental observations of Schubauer and Klebanoff (1956), Klebanoff, Tidstrom and Sargent (192), Gregory and Walker (1956) as reported by Sedney (1973), Mochizuki (1961), Tani et al (1962), Taneda (1956), Magarvey and Bishop (1961), Magarvey and MacLatchy (1962), Achenbach (1972), Wygnanski et al (1976, 1979), and the present series of experimental results, an

attempt is made to construct the sequence of events which lead to transition in the wake of a circular cylinder attached to a flat plate.

We consider the present experimental set up with fixed height and diameter of circular cylinder located at a fixed distance from the leading edge of the flat plate. The free stream wind speed is varied to change to Reynolds number of the flow. Furthermore, it is assumed that the wake of an attached circular cylinder of equal diameter and height will not be basically different from the wake of an attached sphere.

(i) At R_k of about 300, the wake consists of a relatively large horseshoe vortex wrapped around the base of the circular cylinder attached to the plate and two thin trailing streamwise vortices located at a height of about $\hat{y} = 1$. the directions of rotation of these two pairs of vortices are like those observed by Gregory and Walker (1956). At this Reynolds number, the wake is steady, laminar and the transition to turbulence has not set in.

(ii) As R_k is increased, the two trailing vortices at $\hat{y} = 1$ are no longer parallel in plan view, but develop an instability resulting in a pattern of the two threads converging and then diverging followed by converging again and so on in a longitudinal chain like pattern, the converging nodal stations having a certain wavelength. In the side view also, each trailing vortex form a kinky wire (like a stretched

soft spring) like line instead of a straight line as in state. (i)

(iii) Further increase in R_k causes the chain like pattern of trailing vortices at $\hat{y} = 1$ to become more unstable and break into laminar vortex ring. As these rings move downstream they diffuse by viscous action. the horseshoe longitudinal vortices attached to the plate seem to remain unaffected. Transition to turbulence has not yet taken place in the wake of the circular cylinder. Further gradual increases in R_k shifts the location of vortex ring formation nearer to the circular cylinder.

(iv) Formation of vortex rings in the outer flow region takes place at a discrete frequency in a manner very similar to the Strouhal number values are close to 0.2 as observed for the sphere in the similar Reynolds number range. Vortex ring shedding in the outer flow region also excites the longitudinal horseshoe vortex structure attached to the flat plate at the same frequency as vortex ring shedding frequency.

(v) From the present data, it appears that the disturbances associated with the vortex ring shedding in the outer region of the attached cylinder wake decay in magnitude, while the induced disturbances in the wall region amplify downstream in the sidelobe regions in the manner similar to the amplification of three dimensional disturbances in the mean velocity valley regions of flat plate boundary layer.

(vi) The present experiments have not located the breakdown region and the birth of turbulent spot location but the present data indicate that it is likely to appear in the wall region perhaps on either side of the center line of the wake. Since, additional adjacent longitudinal vortices attached to the plate ar created as the disturbed flow proceeds downstream, it is also possible that additional breakdowns of laminar flow take place along the edge of the turbulent wedge in a continuing manner.

(vii) At sufficiently high Reynolds number subsequently,the vortex ring shedding structure in the outer region may also undergo transition to turbulence in a manner similar to the conventional wake of sphere in uniform flow undergoing ransition. Even at Reynolds number high enough to attach turbulence to the circular cylinder it seems that the turbulence will originate in the wall region due to immediate breakdown of flow on either side of the cylinder wake axis, because the laminar vortex ring shedding in sphere wake continues at Reynolds number much higher than the value of 1000 as observed by Achenbach (1972). Finally it is believed that the local Reynolds number based on displacement thickness may have a critical value that may control the breakdown of flow in wall laminar shear layers with or without artificial tripping devices.

The author wishes to acknowledge the discussions with Dr.M.M. Oberai of Mechanical engineering, the assistance of Mr. S.N. Singh of Applied Mechanics, IIT Delhi in collecting data, the help of Mr. J.K. Prasad of Aerodynamics Division, V.S.S.C. Trivandrum, Mr. R. Krishnamurthy, Mr. K.S. Mudddappa, Mr. P.R. Choudhary, Mr. S.C.M.Yadav and Mr.V.N. Pandey at various stages of experimental program. This work was sponsored by the Aerodynamics Panel of Aeronautics R & D Board through a grants - in aid-scheme during 1978-80. This report was prepared in 1980-81.

References

Achenbach, E. 1972 **J. Fluid Mech. 62**, 209-221

Benney, D.J. & Lin, C.C. 1960 **Phys. Fluids 4**, 656-657

Dryden, H.L. 1953 **J. Aero. Sci. 20**, 477-482.

Emmons, H.W. 1951 **J. Aero. Sci. 18**, 490-498.

Gregory, N. & Walker, W.S. 1956 ARC R & M No. 2779

Gupta A.K. 1980 **Phys. Fluids 23**, 221-223

Gupta A.K. 1980 Paper presented at XVth Int. Cong. Theoretical & Applied Mechs. Toronto, Canada.

Gupta A.K. & Singh S.N. 1979 Aero. Engg. IIT Kanpur, Technical Report AE-24/79

Hall G.R. 1967 **AIAA Journal, 5**, 1386-1392

Klebanoff P.S., Schubauer, G.B., & Tidstrom K.D. 1955, **J. Aero. Sci. 22**, 803-804

Klebanoff P.S. Tidstrom K.D., & Sargent L.M. 1962 **J. Fluid Mech. 12**, 1-34

Klebanoff P.S., & Tidstrom K.D. 1972 **Phys. Fluids 15**, 1173-1188.

Magarvey R.H., & Bishop, R.L. 1961 **Can. J. Phys. 39**, 1418-1442.

Magarvey R.H., & MacLatchy, C.S. 1965, **Can. J. Phys 43**, 1649-1656

Mochizuki, M. 1961 **J. Phy. Soc. Japan. 16**, 995-1008.

Potter, J.L. 1957, **J. Aero. Sci. 24**, 158-159.

Schlichting, H. 1960 **Boundary Layer Theory**, McGraw Hill, 4th edition.

Schubauer, G.B., Skramstad, H.K. 1947 N.A.C.A. Report 909

Schubauer, G.B., & Klebanoff, P.S. 1956 N.A.C.A. Report 1289

Sedney, R. 1973 **AIAA Journal 11**, 782-792.

Smith A.M.O. & Clutter, D.W. 1959 **J. Aero. Sci. 26**, 229-245

Taneda, S. 1956 **J. Phys. Soc. Japan 11**, 1104-1108

Tani, I., Komoda, H., Komatsu, Y., & Iuchi, M. 1962 Aeronautics

Research Institute, University of Tokyo Report 735.

Tani, I. 1969 **Ann. Rev. Fluid Mech. 1**, 169-196.

Wygnanski, I., Sokolov, M. & Friedman, D. 1976 **J. Fluid Mech. 78** 785-819.

Wygnanski, I., Haritonidis, J.H. & Kaplan, R.E.1979 **J. Fluid Mech. 92**, 505-528.

List of Figures

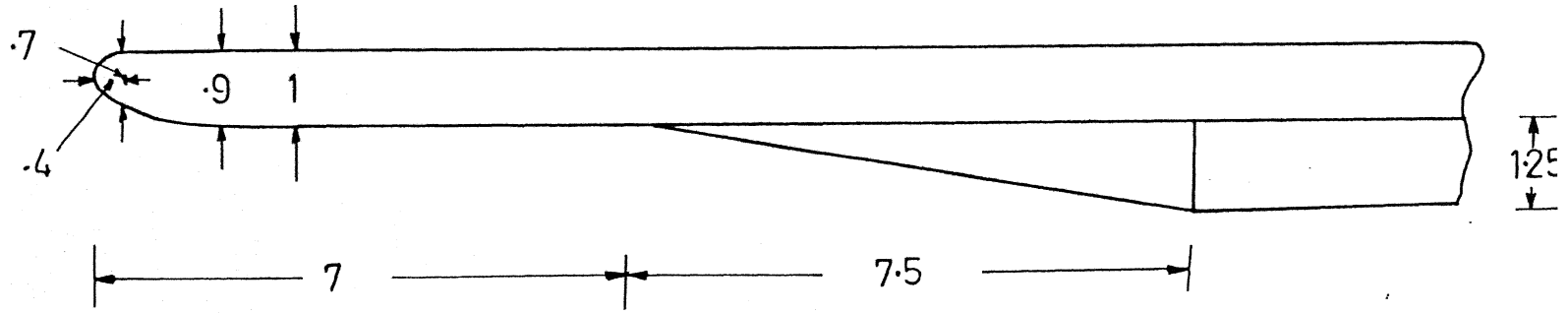

(a) Leading edge detail

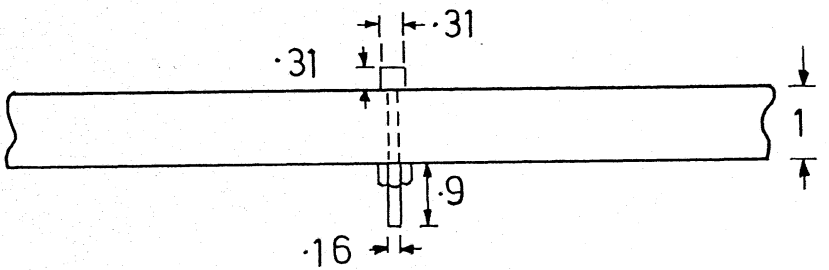

(b) Tripping device mounting

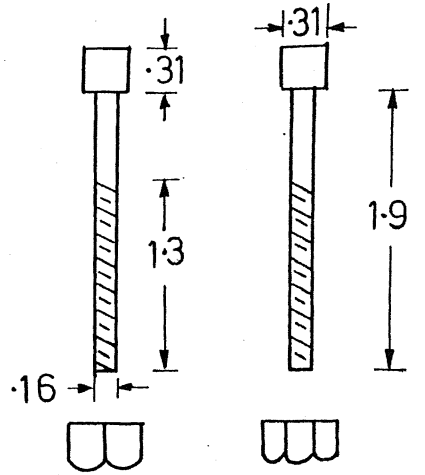

(c) Tripping device (brass)

All dimensions in cm

FIG. 1 DETAILS OF FLAT PLATE LEADING EDGE AND THE TRIPPING DEVICE

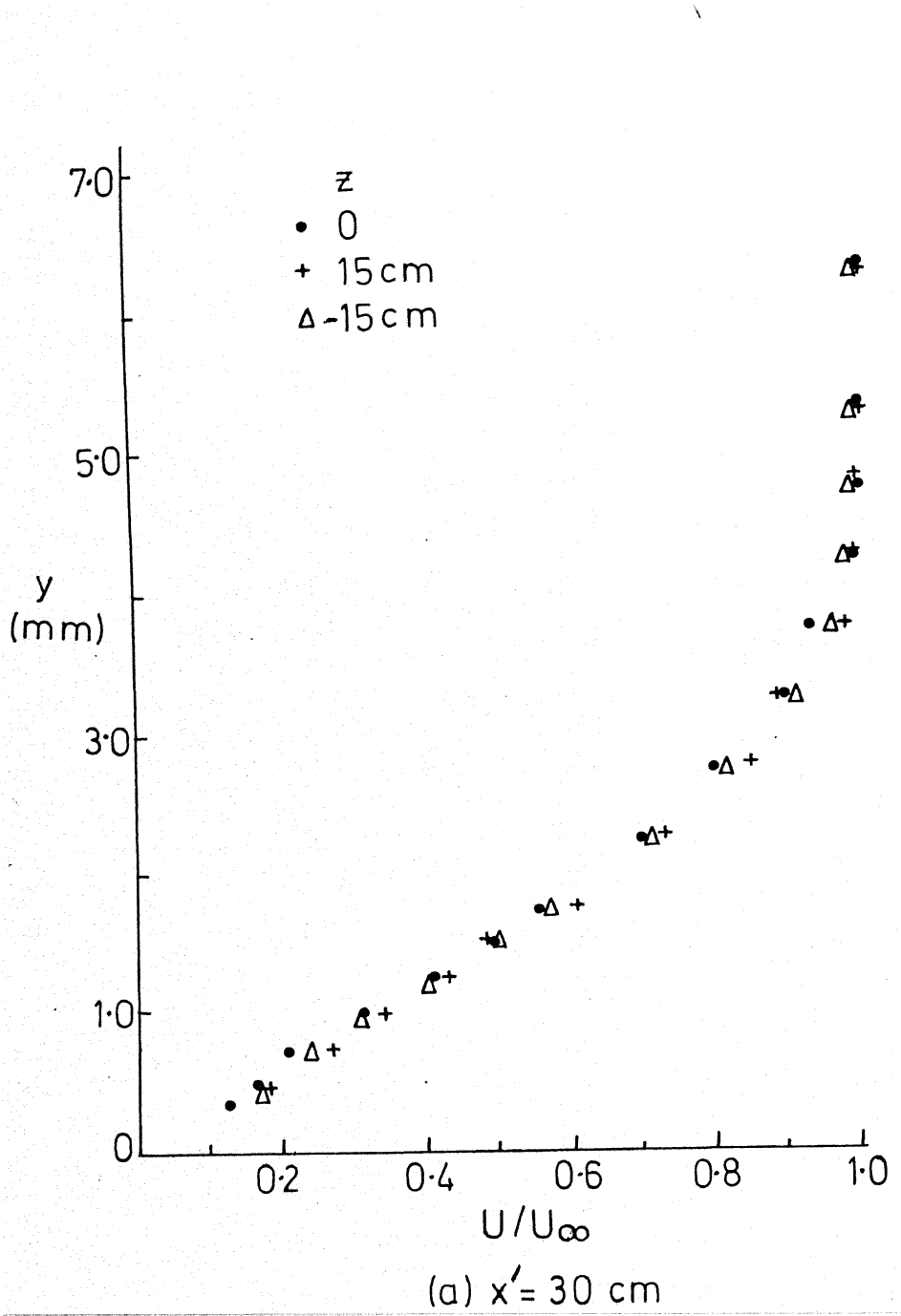

(a) $x' = 30$ cm

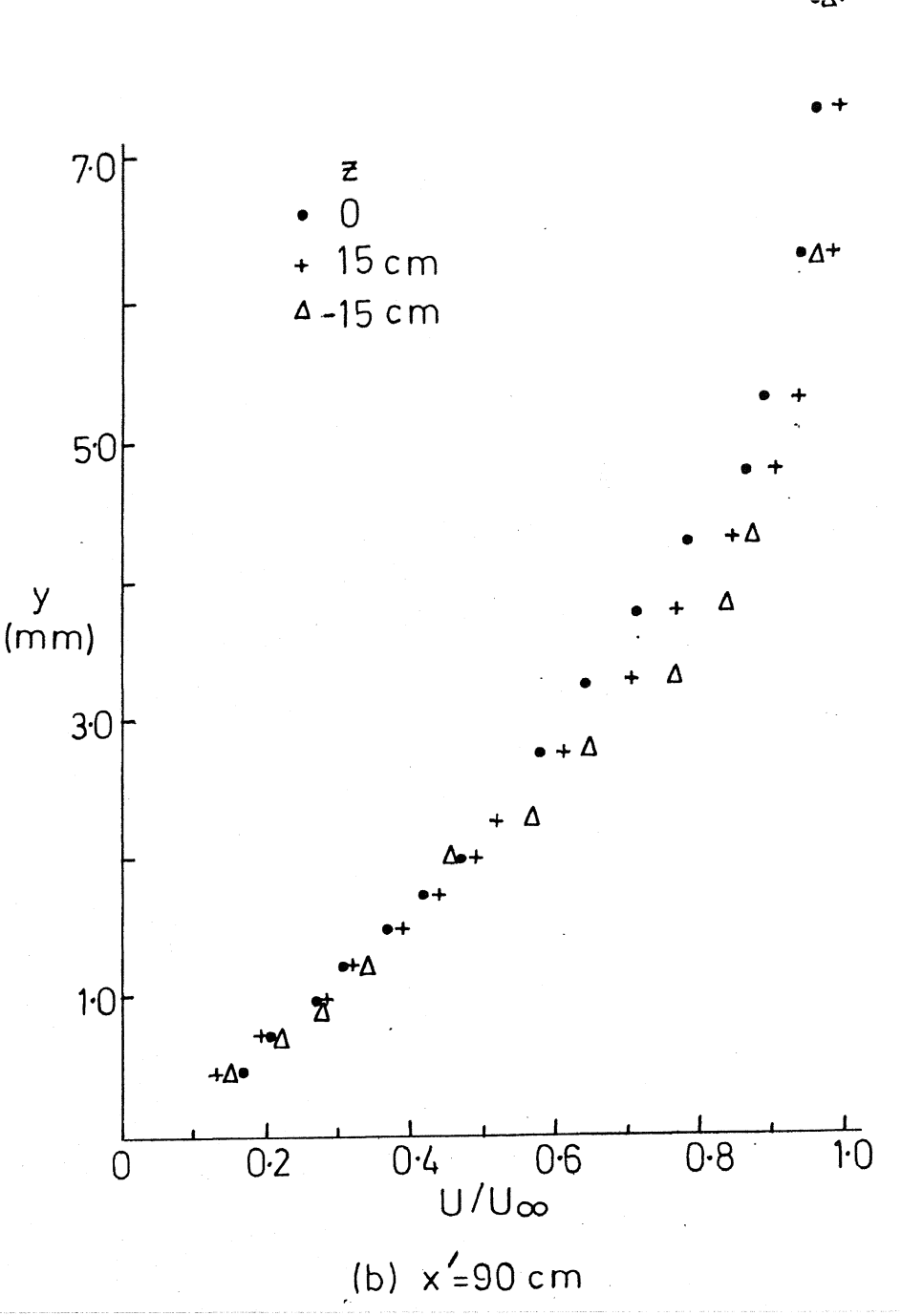

(b) $x' = 90$ cm

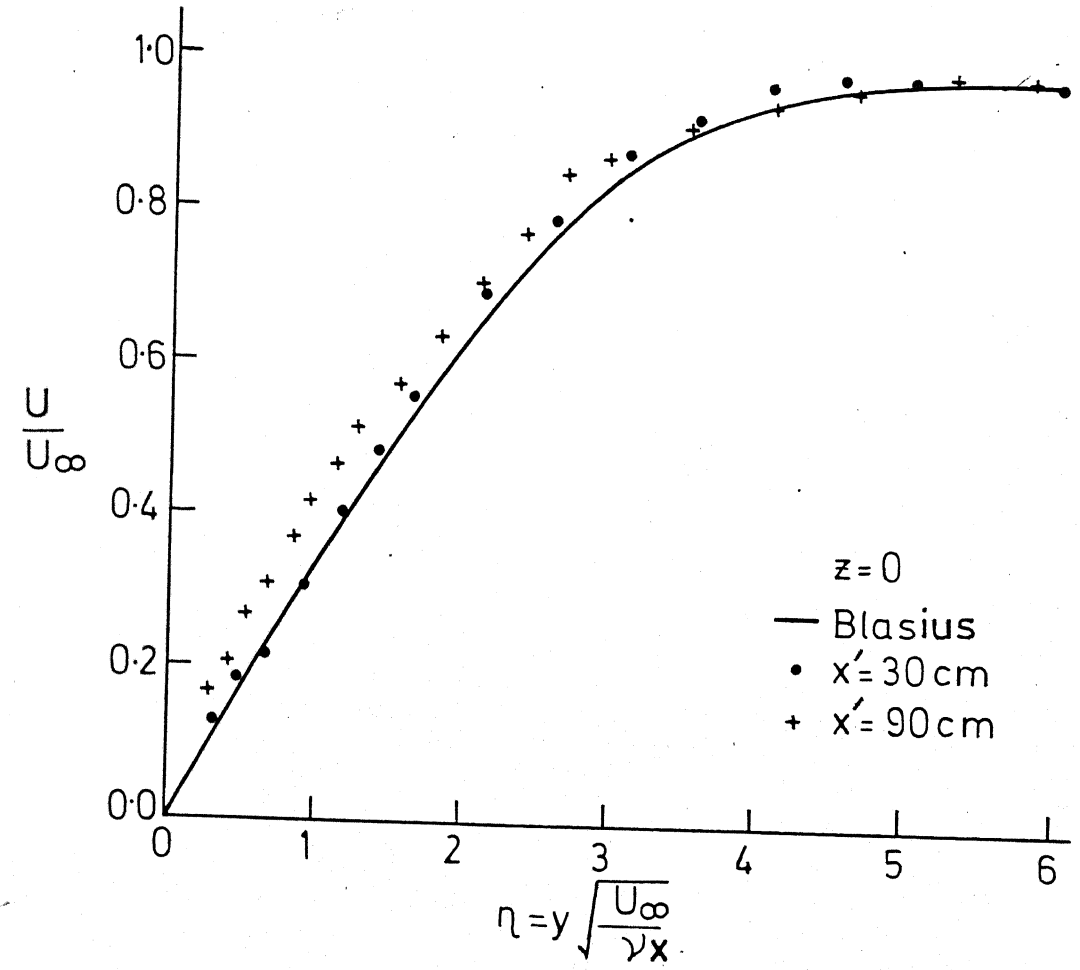

FIG. 3 MEAN VELOCITY PROFILES ON CLEAN PLATE PLOTTED IN BLASIUS COORDINATES
$U_\infty/\nu = 2{\cdot}6 \times 10^5$ per meter

x	Sensitivity
1	0.05 V/cm
2	0.05 V/cm
3	0.05 V/cm
6	0.1 V/cm
8	0.1 V/cm

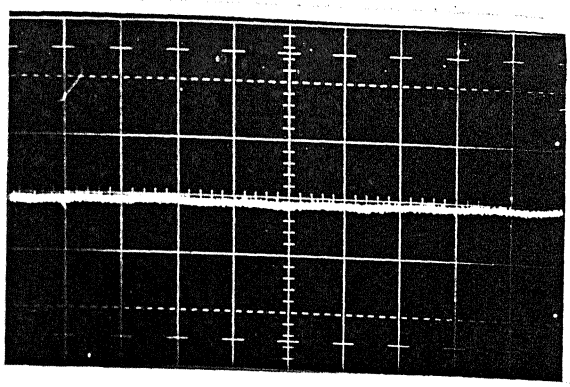

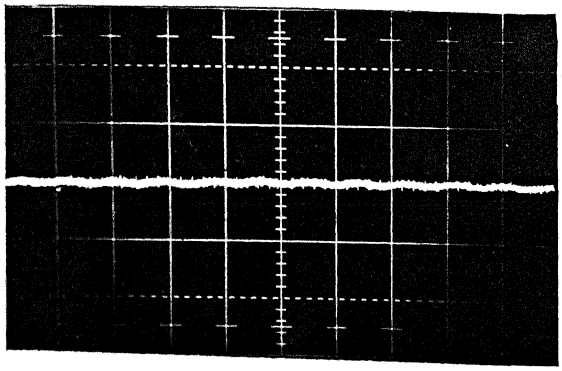

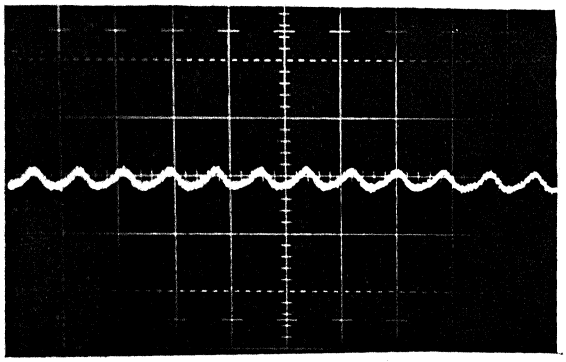

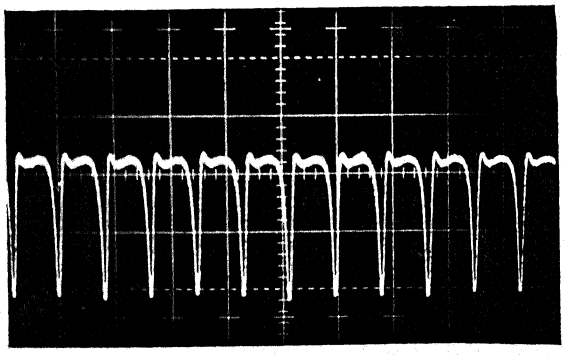

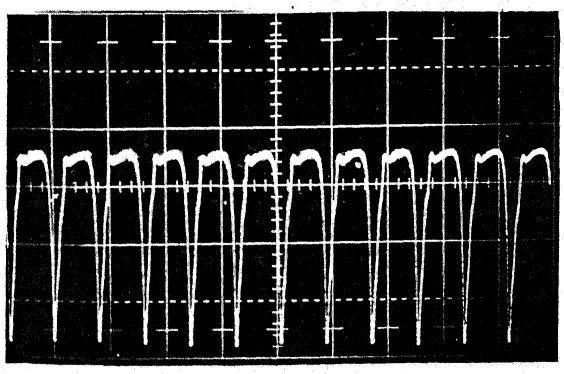

x	Sensitivity
12	0.1 V/cm
16	0.1 V/cm
20	0.2 V/cm
32	0.1 V/cm
40	0.1 V/cm

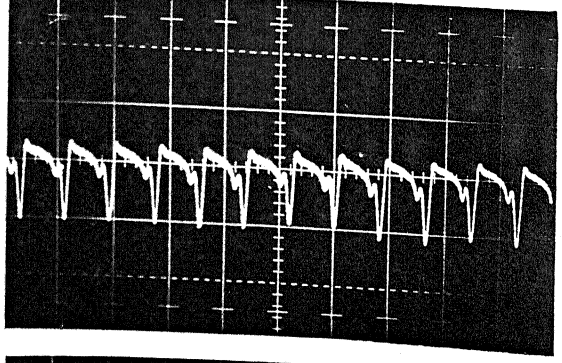

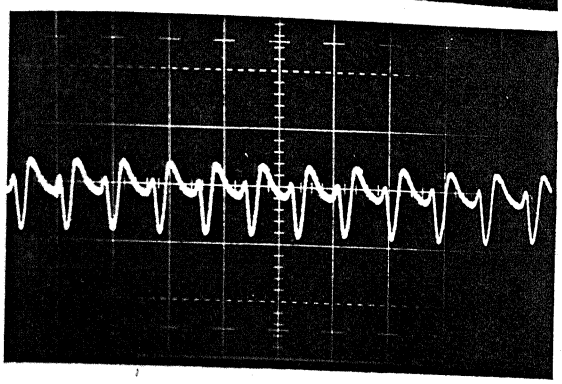

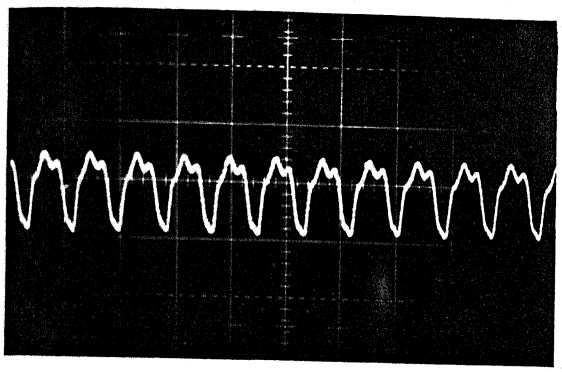

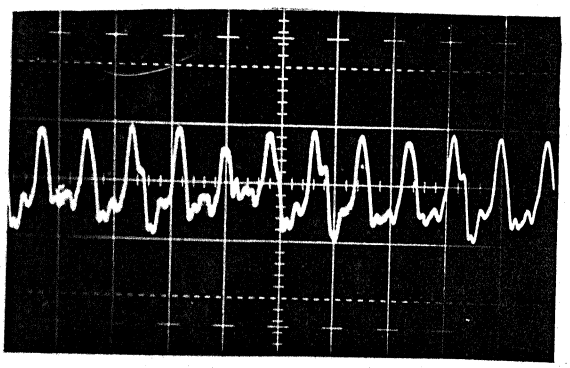

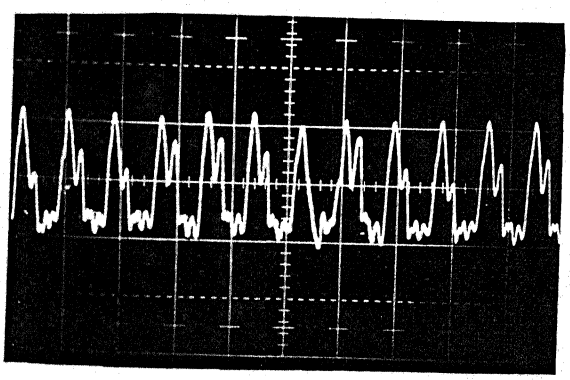

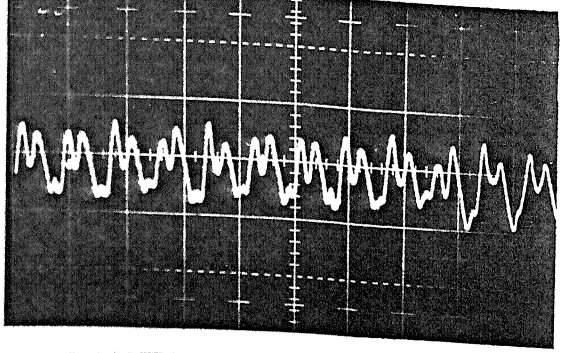

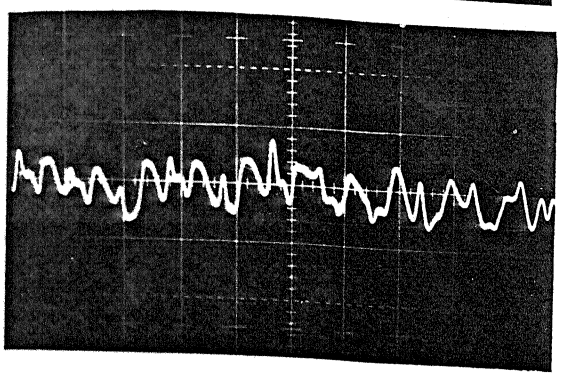

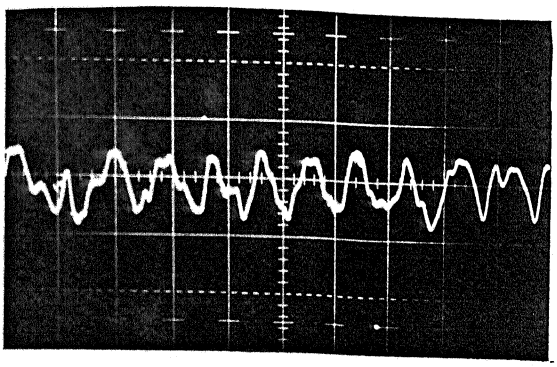

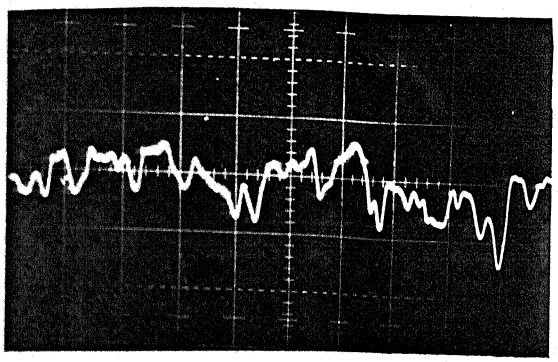

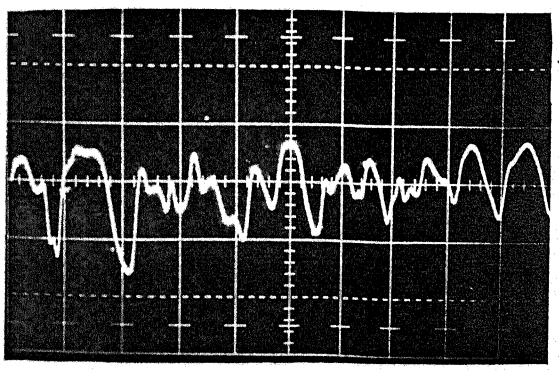

H	Sensitivity
48	0.1 V/cm
56	0.2 V/cm
64	0.2 V/cm
72	0.2 V/cm
80	0.2 V/cm.

Fig. 4 Concluded

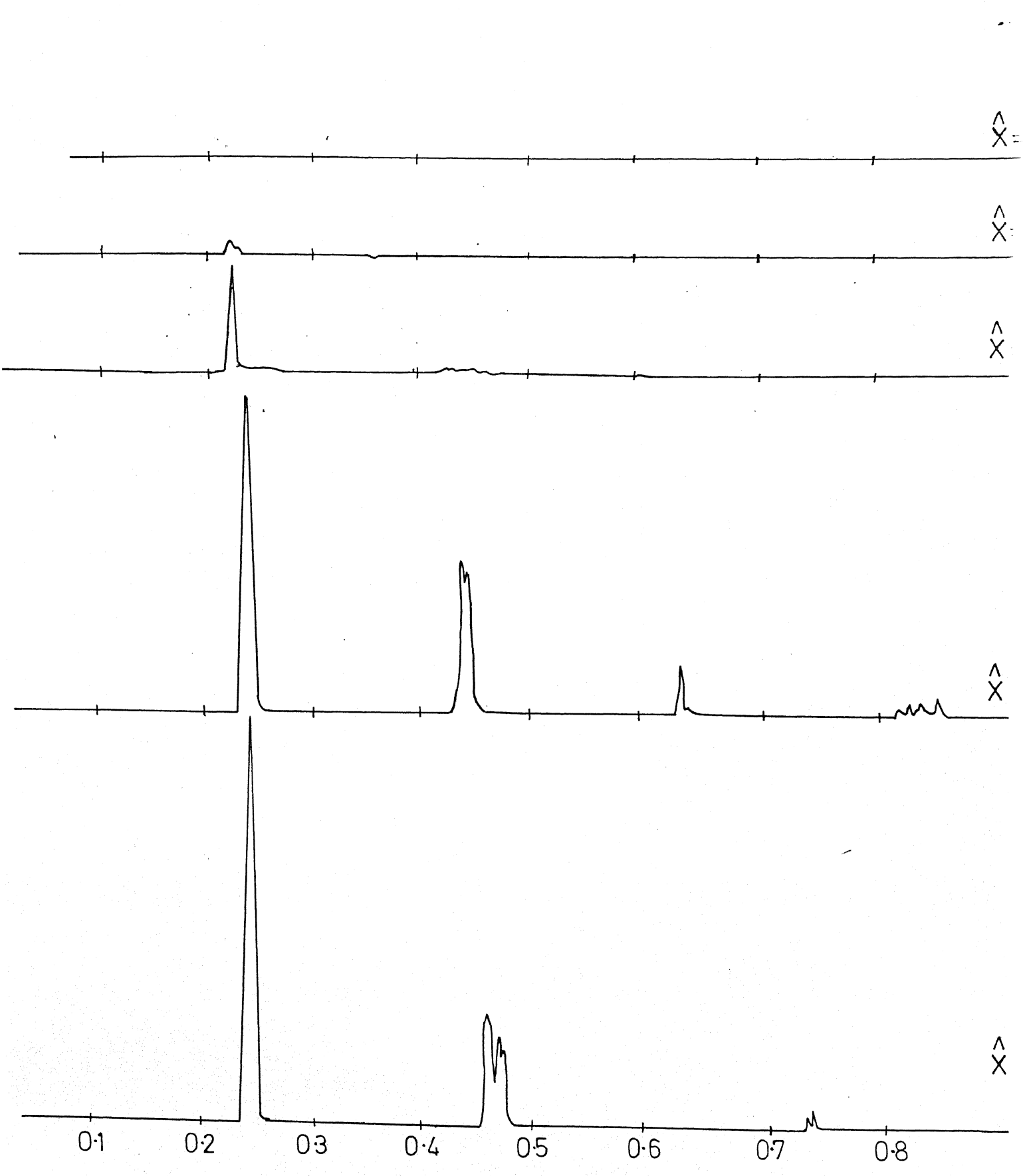

FIG. 5 SPECTRA OF u′ FLUCTUATIONS U_∞=4·1 m/s; $\hat{y}$=1·0; $\hat{z}$=0·0

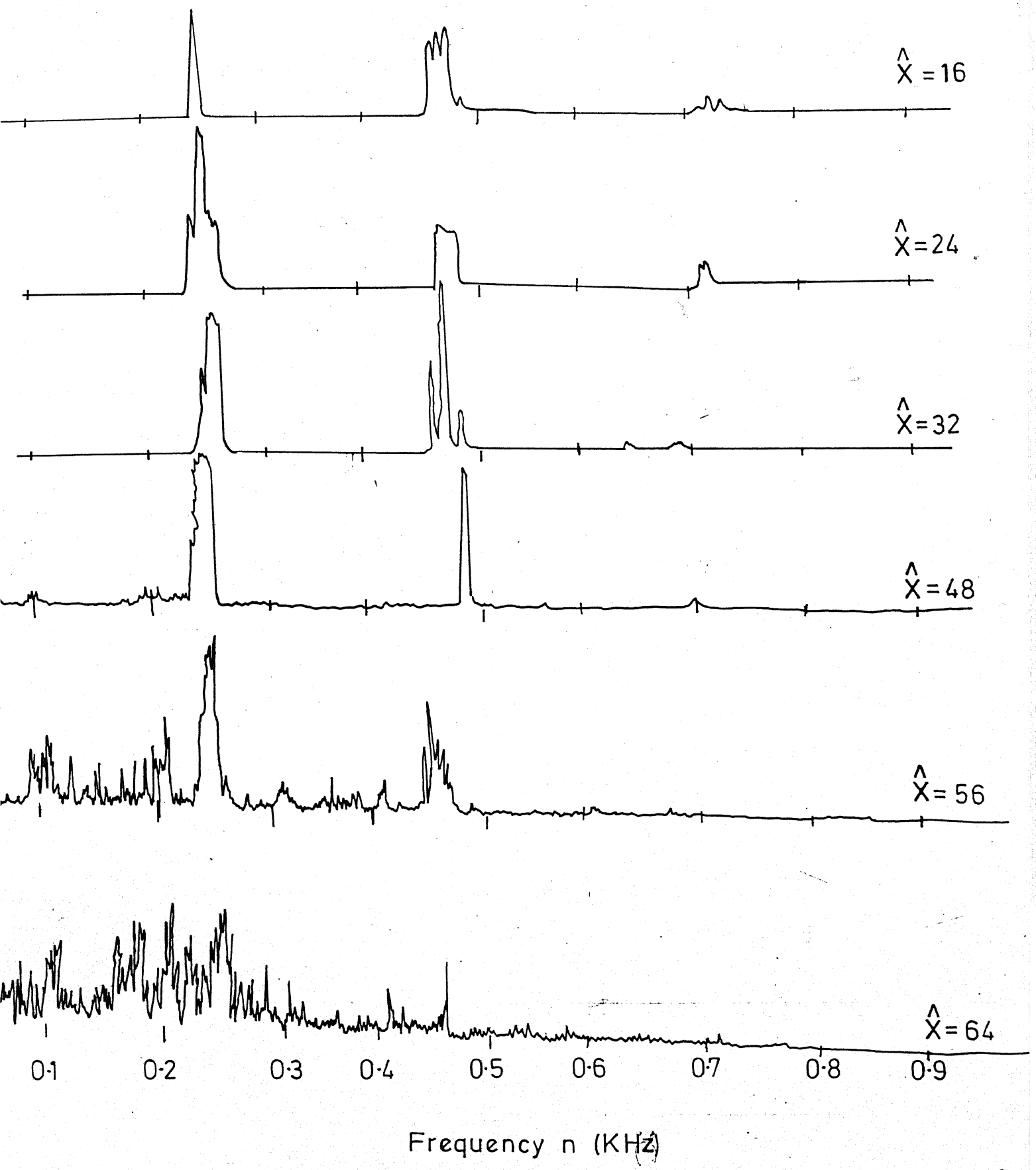

FIG.5 SPECTRA OF u′ FLUCTUATIONS $U_\infty = 4{\cdot}1$ m/s; $\hat{y} = 1{\cdot}0$; $\hat{z} = 0{\cdot}0$

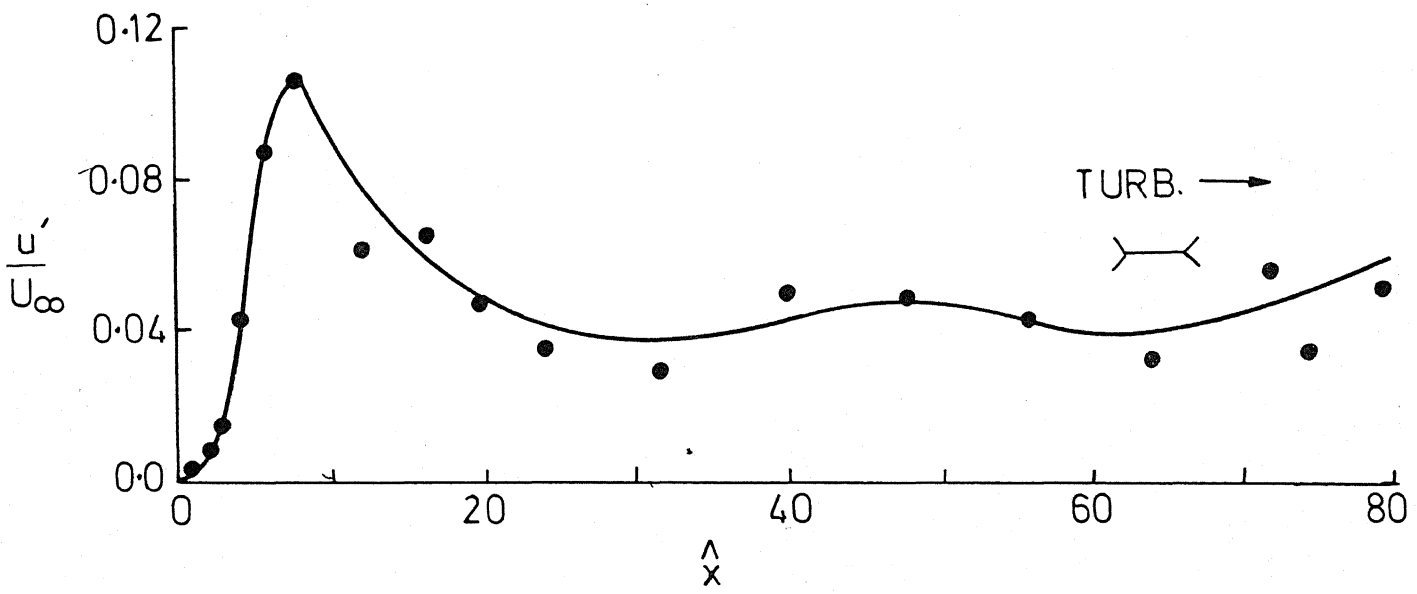

FIG·6 DISTURBANCE INTENSITY DISTRIBUTION
$\hat{y} = 1{\cdot}0$, $\hat{z} = 0{\cdot}0$, $U_\infty = 4{\cdot}1$ m/s , $x'_k = 30$ cm

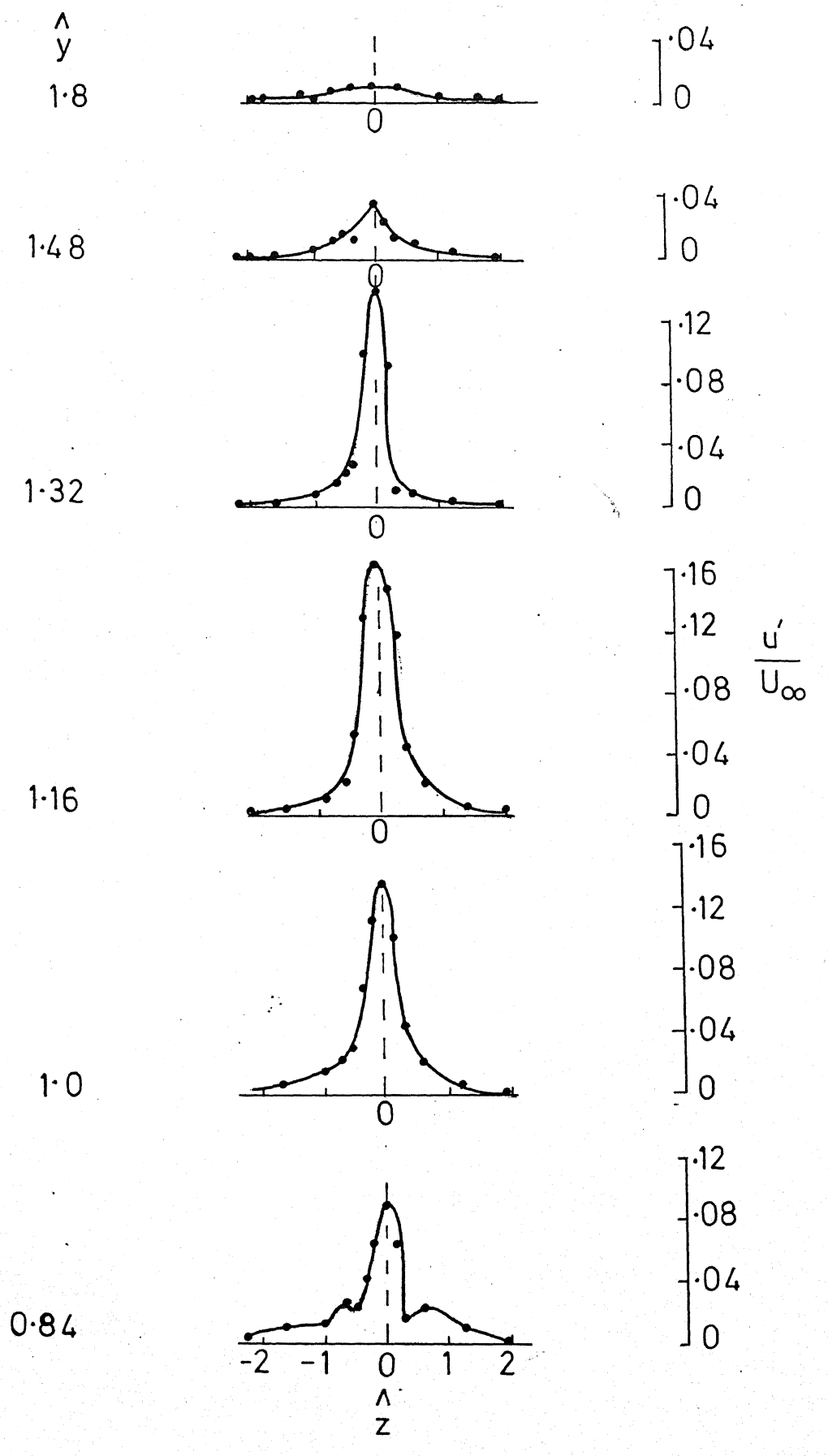

FIG.7 STREAMWISE DISTURBANCE INTENSITY DISTRIBUTION AS A FUNCTION OF $\hat{z}$; $\hat{x}$=8·0

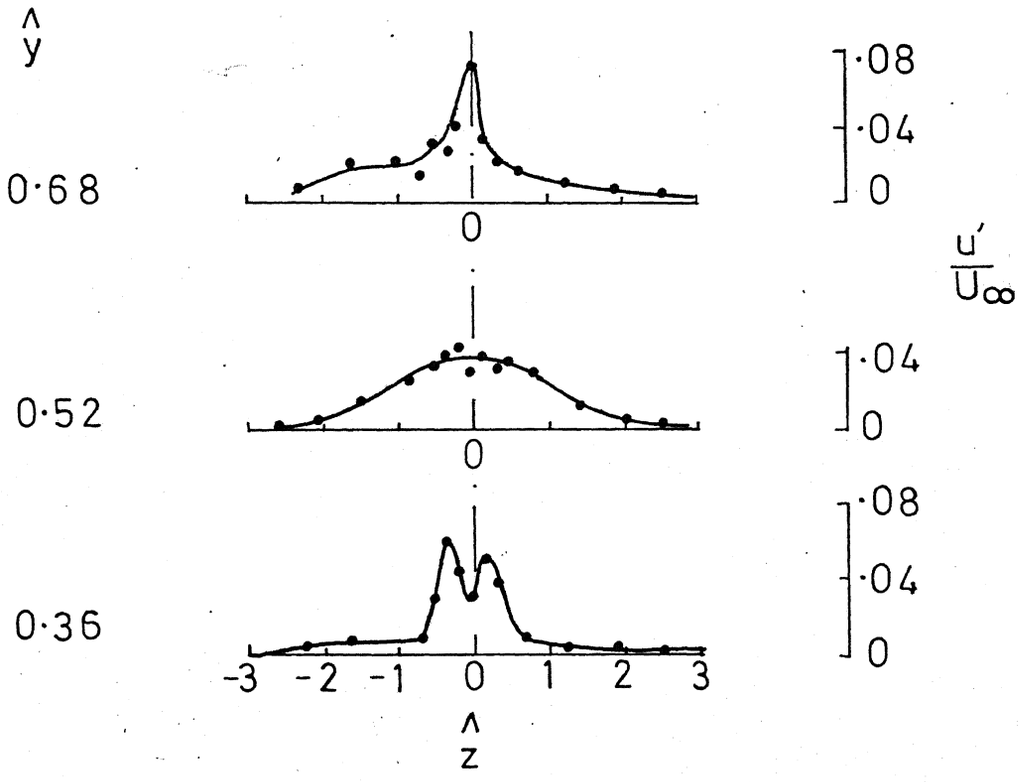

FIG.7 CONCLUDED

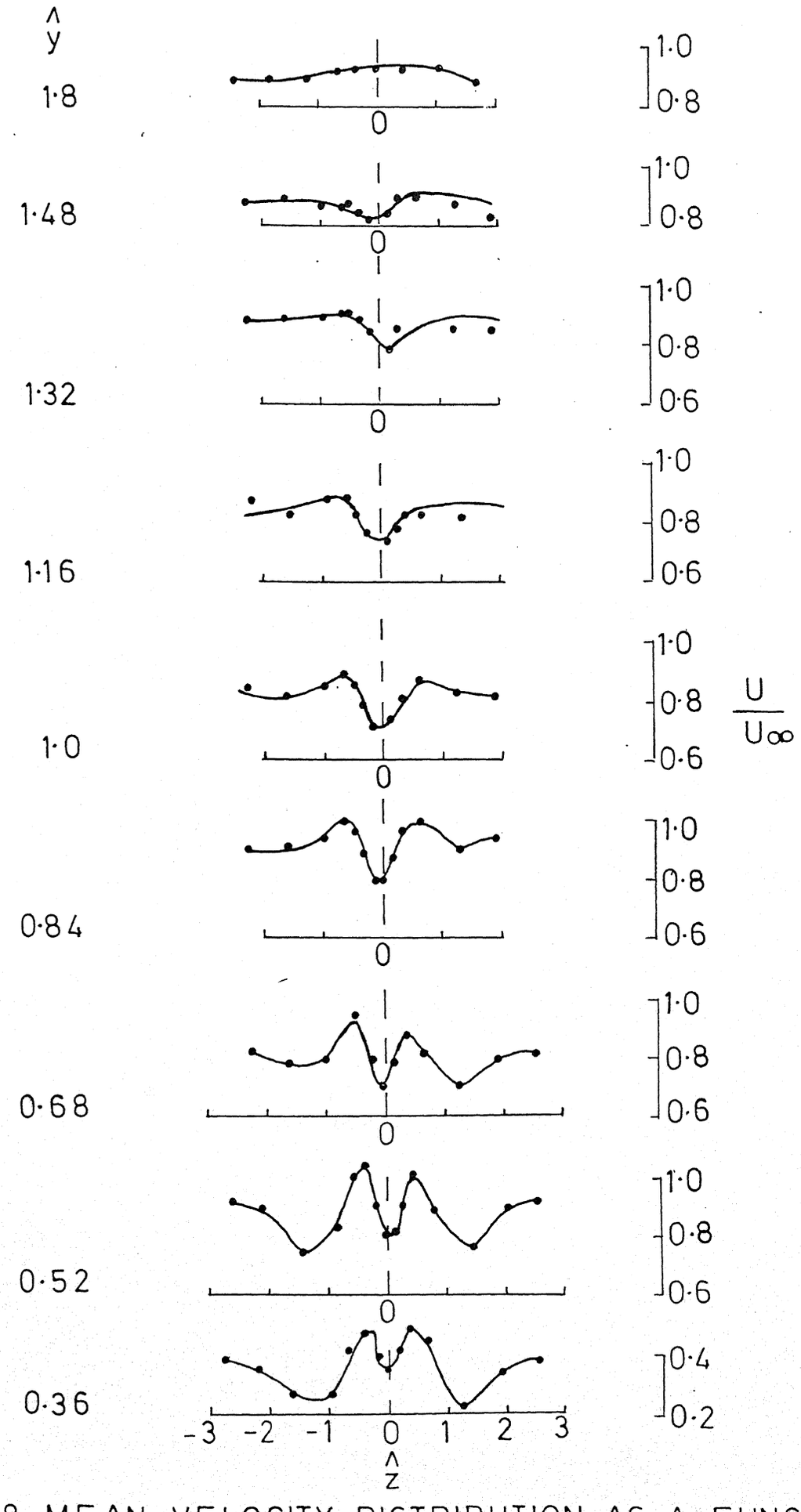

FIG·8 MEAN VELOCITY DISTRIBUTION AS A FUNCTION OF $\hat{z}$. $\hat{x}$ = 8·0

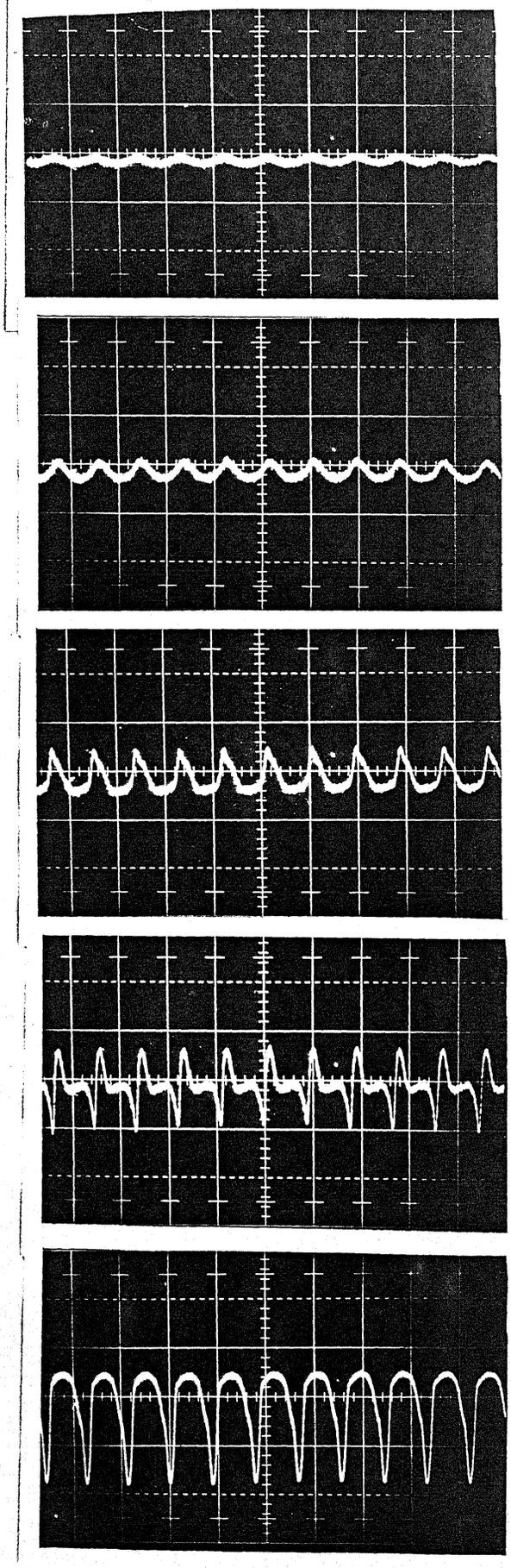

$\hat{y}$	Sensitivity
2.6	0.05 V/cm
1.96	0.05 V/cm
1.48	0.05 V/cm
1.16	0.05 V/cm
0.84	0.05 V/cm

Fig.9 Hot wire traces at $\hat{z}$=0 ; $\hat{x}$ = 8.0 ; sweep 5 ms/cm.

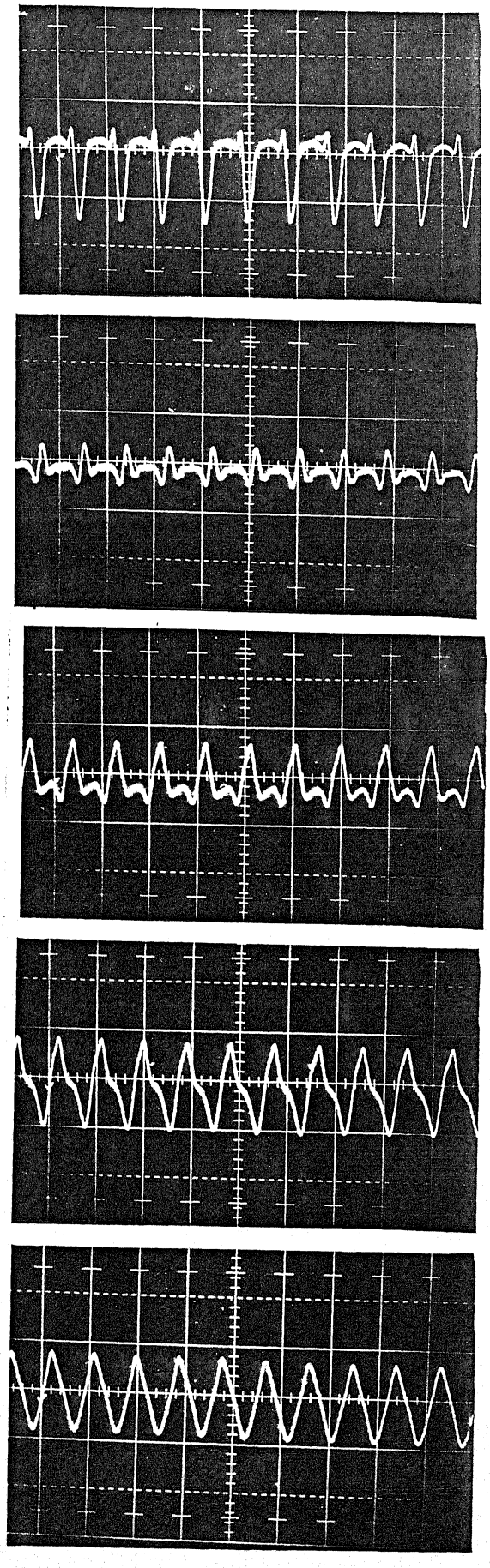

$\hat{y}$	Sensitivity
0.68	0. 1 V/cm.
0.52	0.1 V/cm.
0.36	0.1 V/cm.
0.2	0.1 V/cm.
0.04	0.1 V/cm.

Fig. 9 concluded.

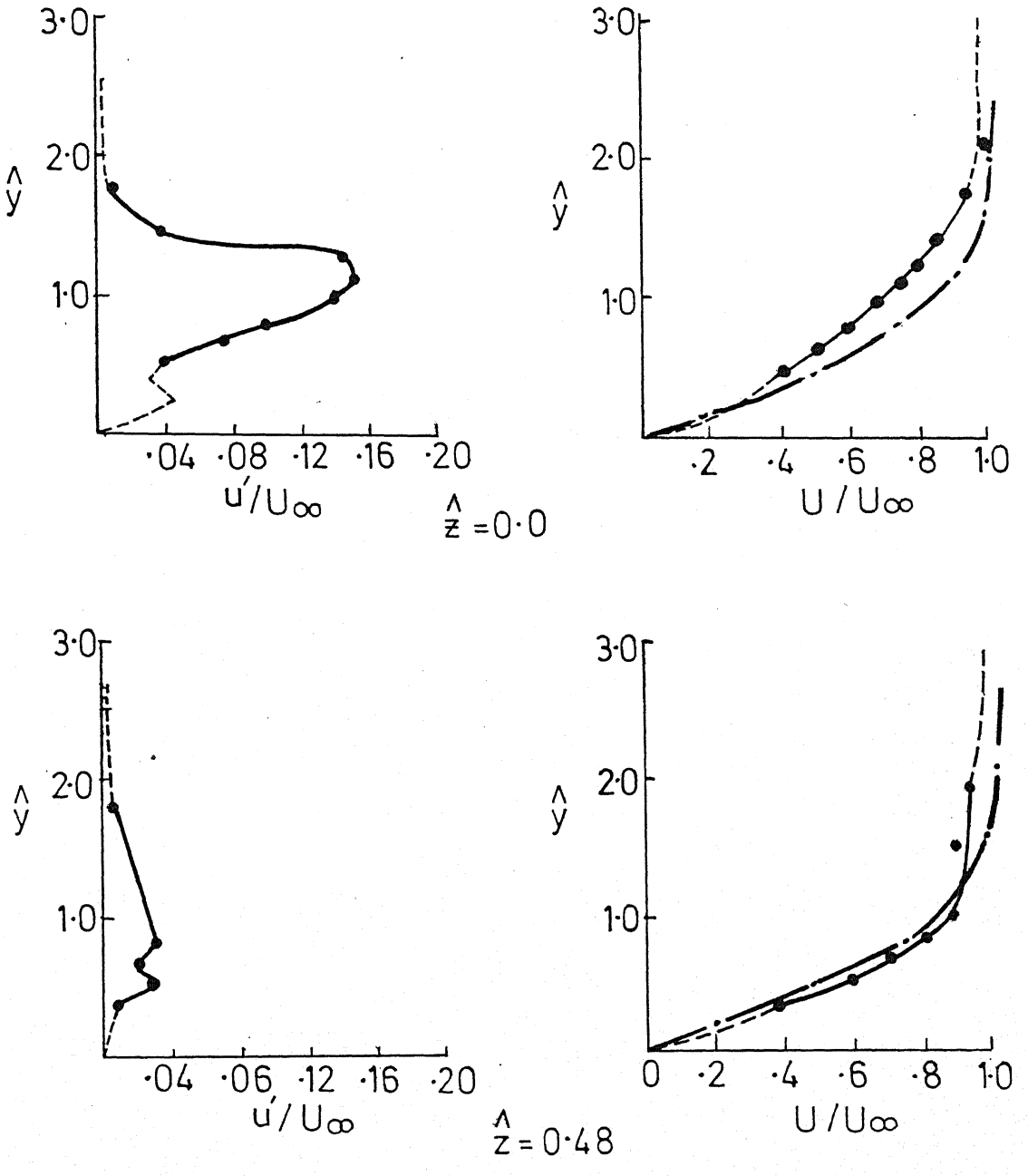

FIG·10 MEAN VELOCITY AND DISTURBANCE INTENSITY PROFILES IN THE $\hat{y}$ DIRECTION

$\hat{x} = 8{\cdot}0$ —·— Blasius

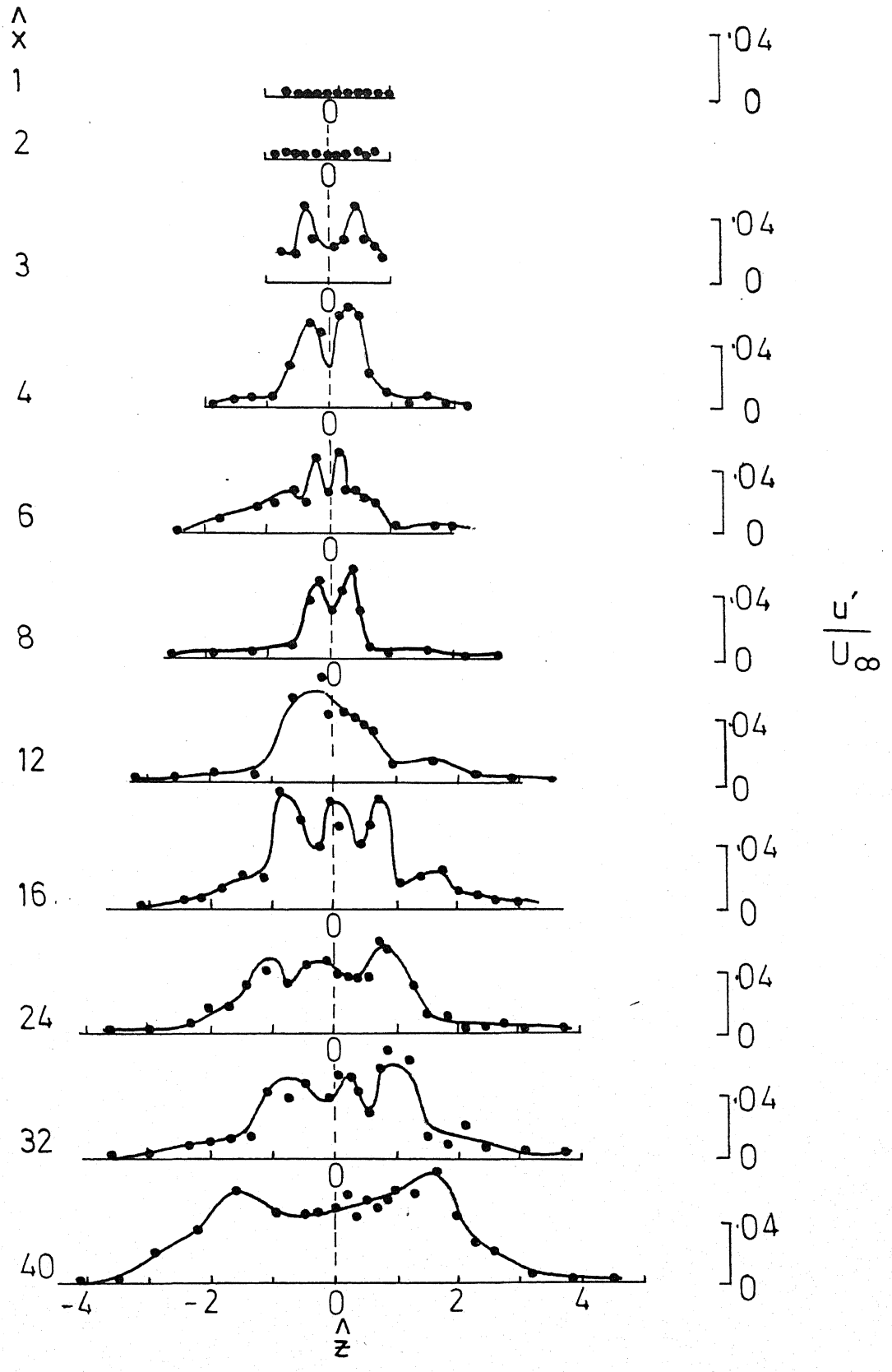

FIG·11 LONGITUDINAL DISTURBANCE INTENSITY DISTRIBUTION IN THE SPANWISE DIRECTION $\hat{Y}$=0·36; INNER LAYER

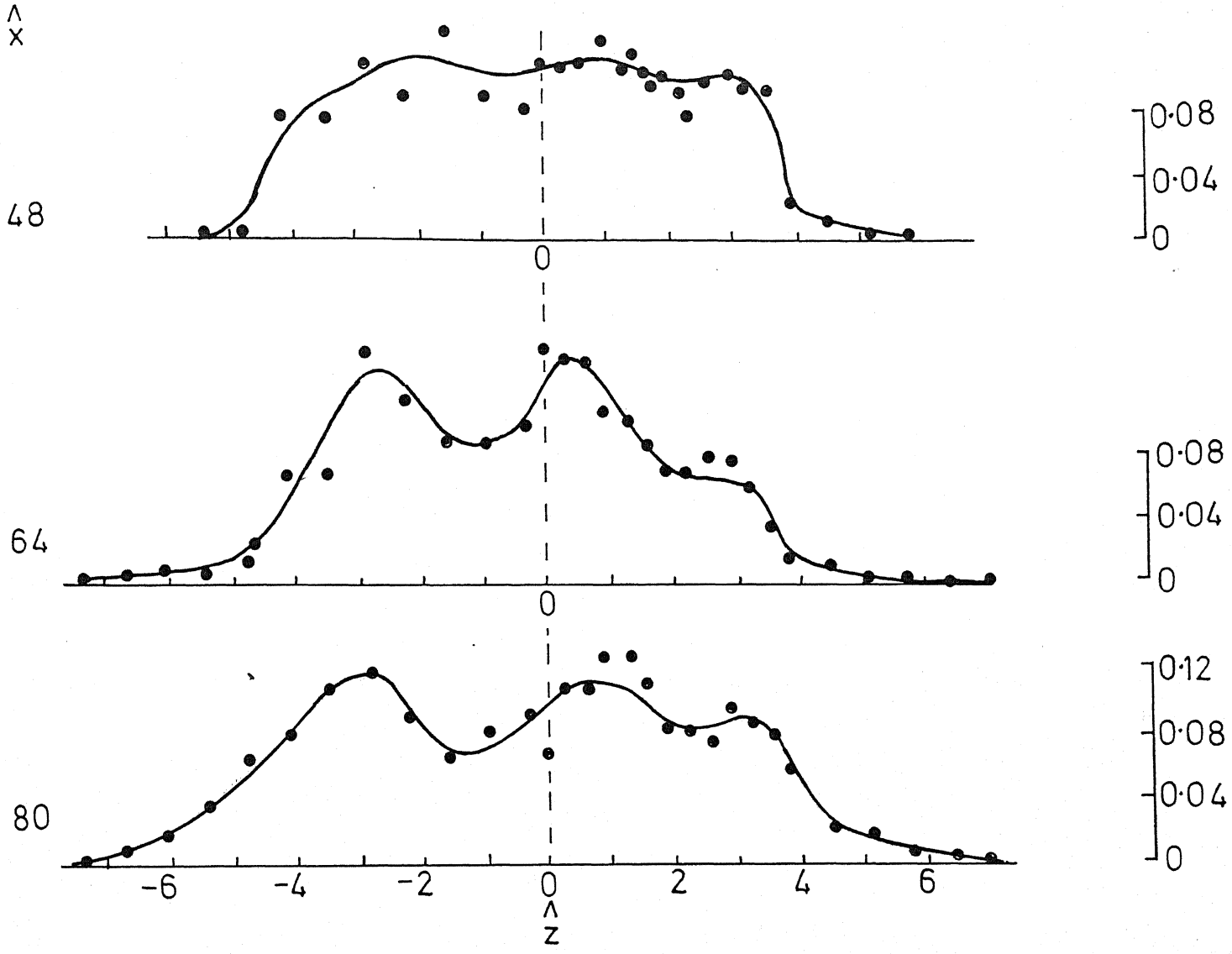

FIG. 11 CONCLUDED

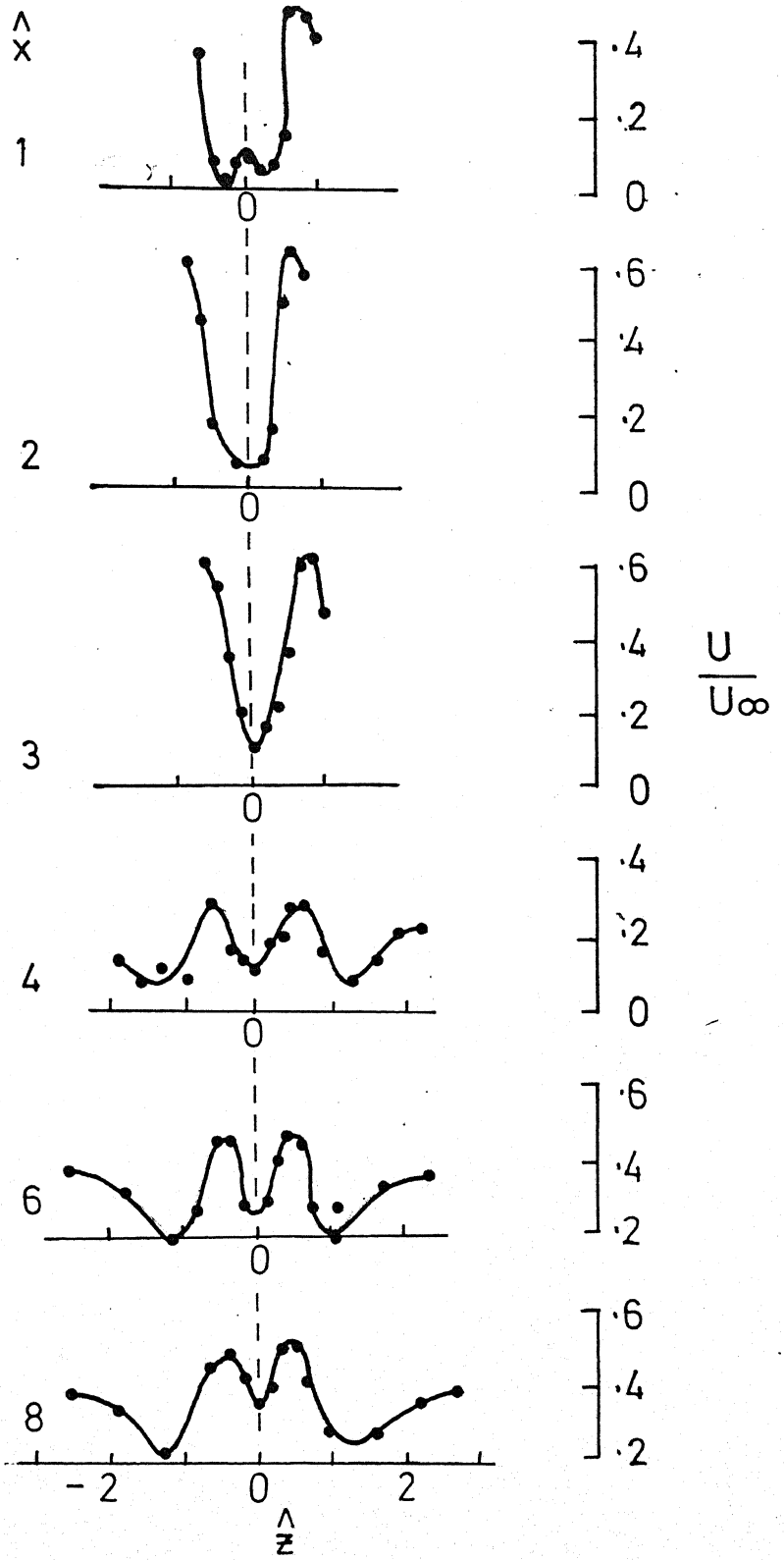

FIG.12 LONGITUDINAL VELOCITY DISTRIBUTION IN THE SPANWISE DIRECTION; $\hat{Y}$=0·36; INNER LAYER

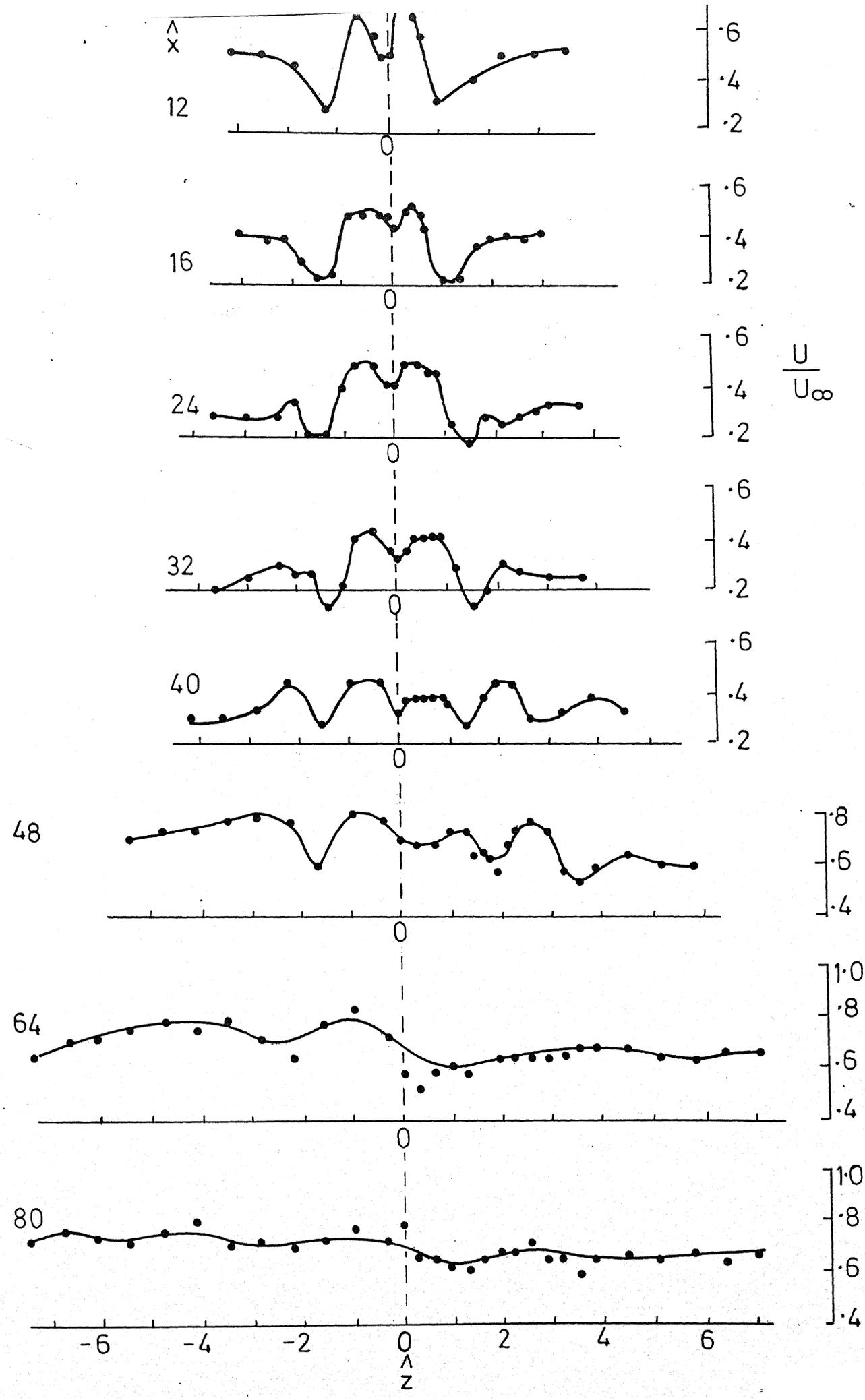
x/c
12
16
24
32
40
48
64
80
0
·6
·4
·2
·8
1·0
U/U∞
-6
-4
-2
2
4
6
z/c

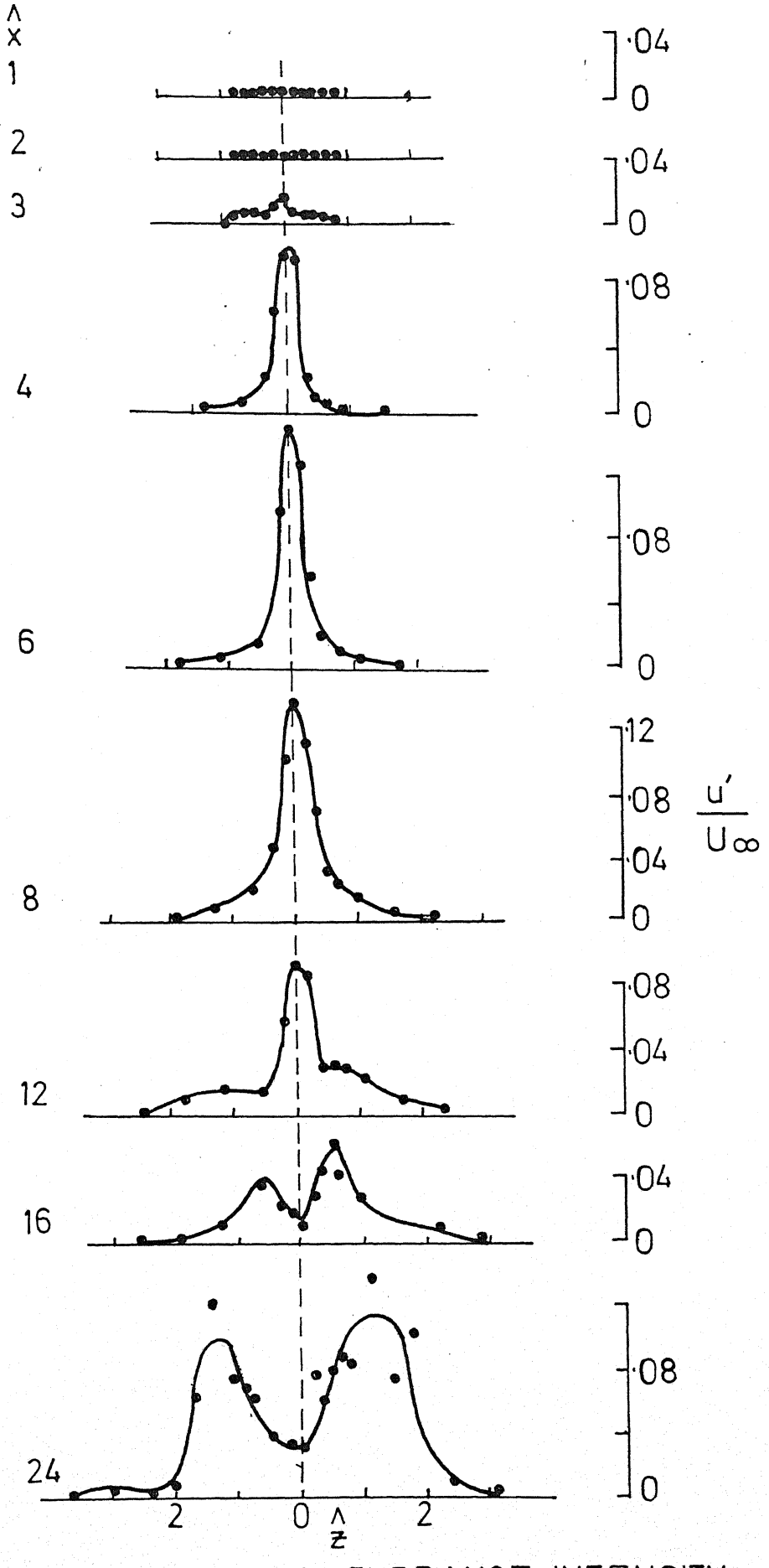

FIG.13 LONGITUDINAL DISTURBANCE INTENSITY DISTRIBUTION IN THE SPANWISE DIRECTION $\hat{Y}$=1·0; OUTER LAYER

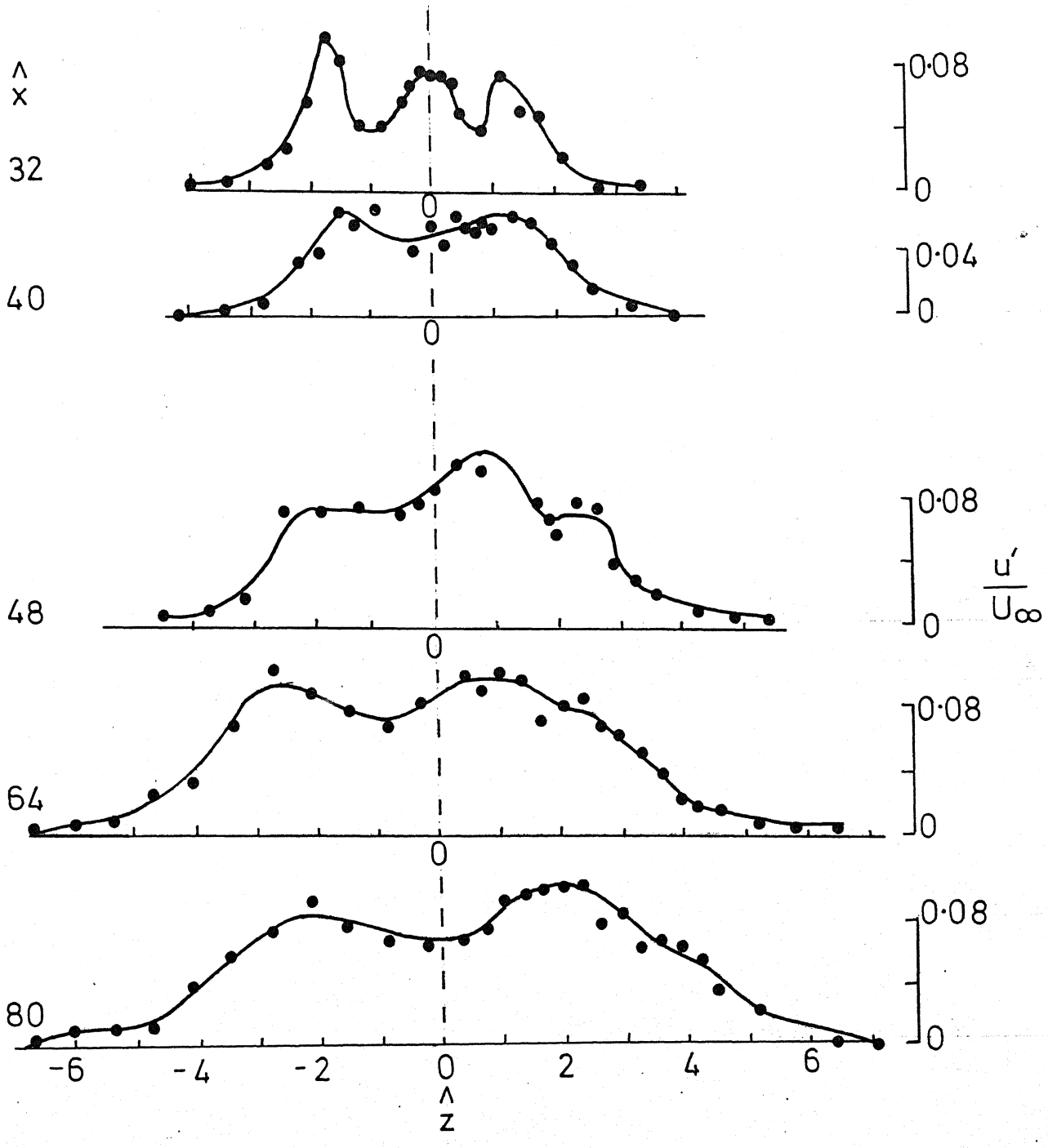

FIG.13 CONCLUDED

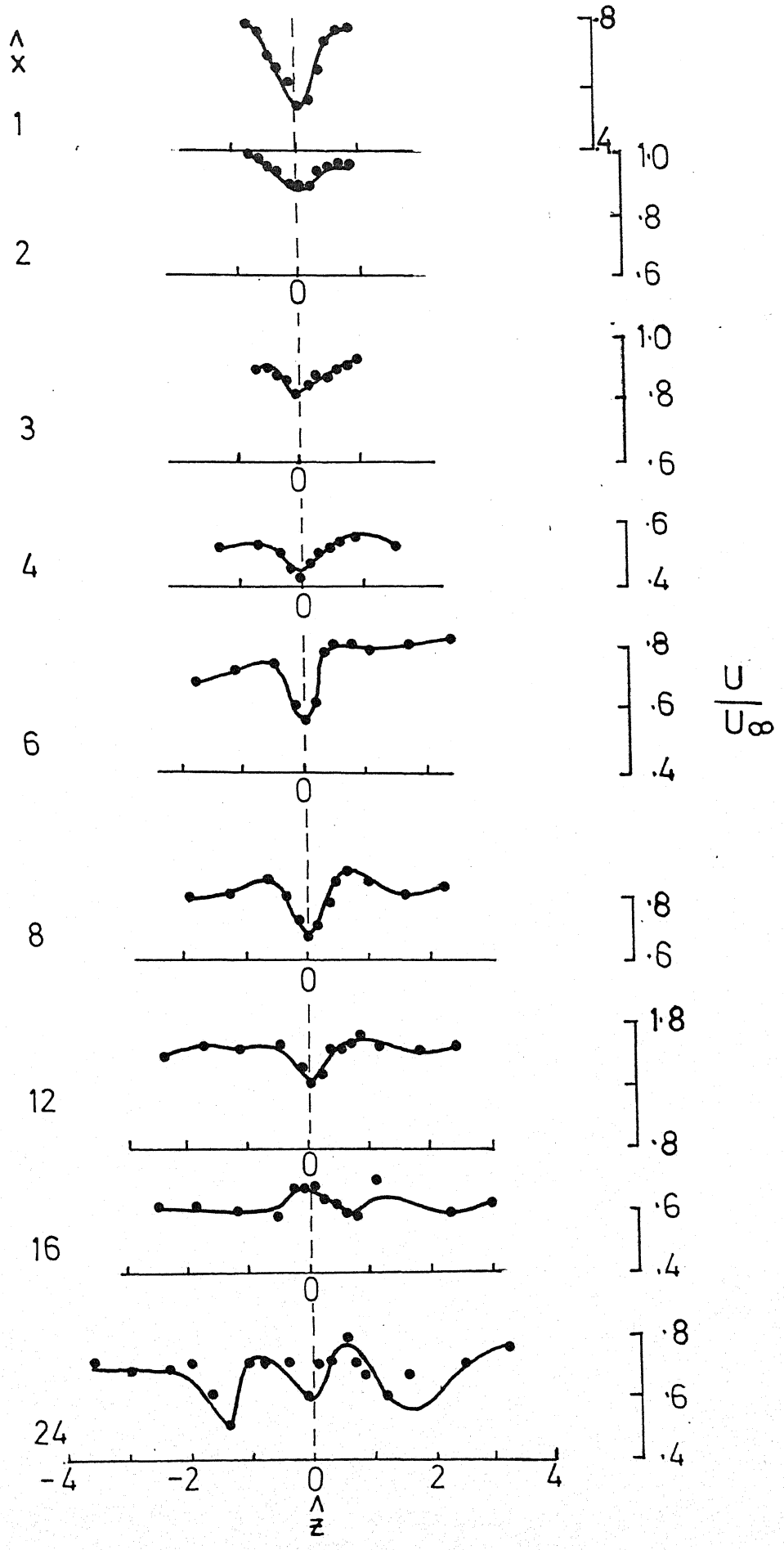

FIG. 14 LONGITUDINAL VELOCITY DISTRIBUTION IN THE SPANWISE DIRECTION; $\hat{Y}$ = 1·0 ; OUTER LAYER

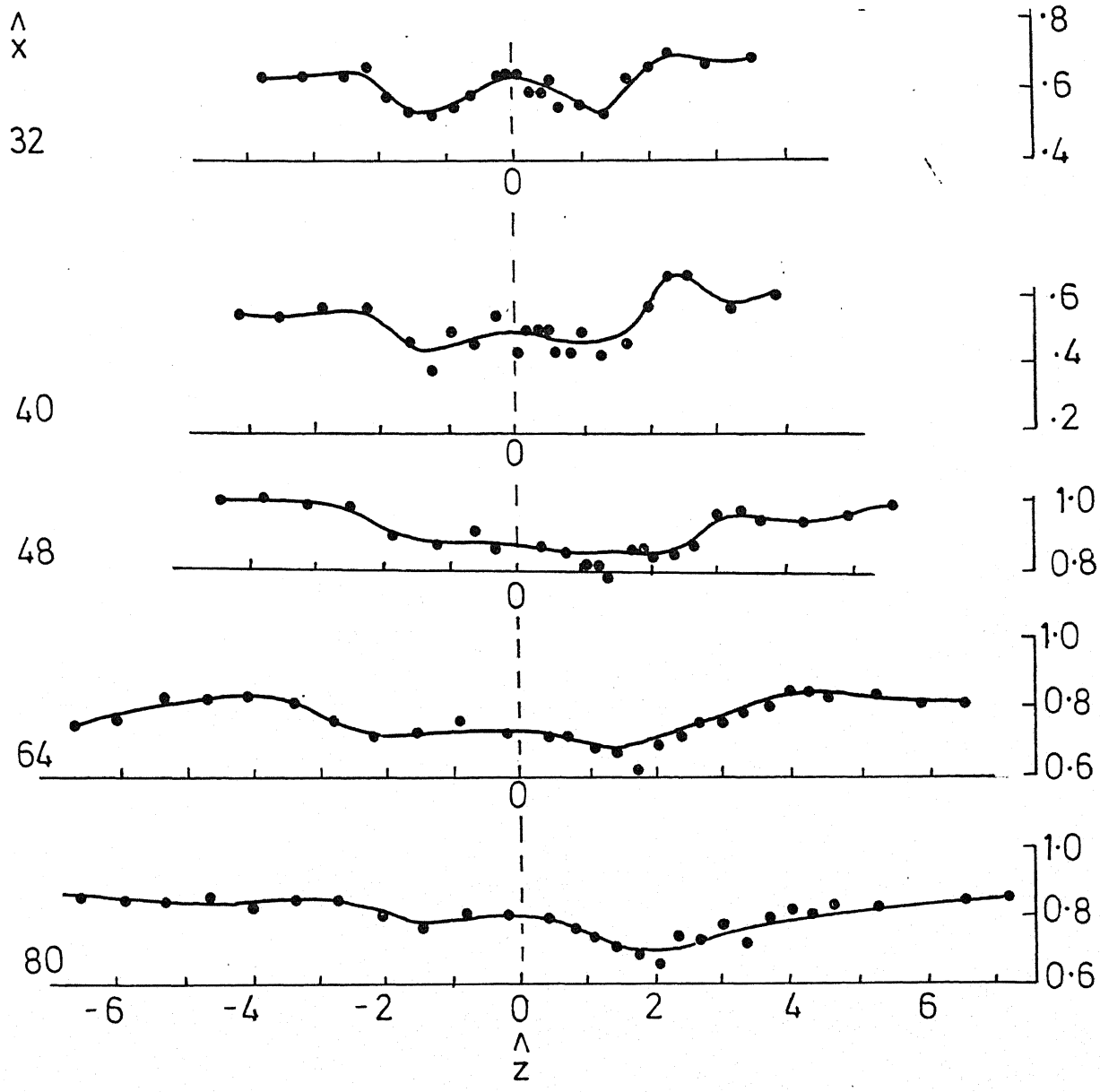

FIG·14 CONCLUDED